CrossMark

Wind and Fire Coupled Modelling—Part II: Good Practice Guidelines

Wojciech Węgrzyński* , Fire Research Department, Building Research Institute (ITB), 1 Filtrowa St., 00-611 Warsaw, Poland
Tomasz Lipecki , Faculty of Civil Engineering and Architecture, Lublin University of Technology, 36 Nadbystrzycka St., 20-618 Lublin, Poland
Grzegorz Krajewski, Fire Research Department, Building Research Institute (ITB), 1 Filtrowa St., 00-611 Warsaw, Poland

Abstract. The requirement to model wind is inherently connected with the modelling of many fire-related phenomena. With its defining influence on fire behaviour, spread and smoke transport, the solution of a problem with and without wind exposure will lead to substantially different results. As wind and fire are phenomena that often require different scales of analysis and approaches to modelling, their coupling is not a trivial task. This paper is the second part of a two-paper review of the coupling between fire safety engineering and computational wind engineering (CWE). Part I contained a review of historical interactions between these disciplines, sorted into six distinct areas: flames, indoor flows, natural ventilators, tunnels, wildfires and urban smoke dispersion. This part of the review contains practical information related to wind modelling in fire analysis, based on various available CWE best practice guidelines. As the authors conclude, the most relevant of these are guidelines related to urban physics and natural ventilation; however, many more are discussed and presented, together with the results of other essential wind engineering experiments and computations. Introduction of wind as a boundary condition is explained in details, both based on wind statistics, or meso/micro scale coupled modelling. The guidelines for wind/fire coupled analyses are subdivided into recommendations for: building the digital domain, spatial and temporal discretisation, the consequences of the choice of a turbulent flow model, and the procedure for optimising CFD analysis of both wind and fire phenomena.

Abbreviations

AIJ   Architectural Institute of Japan
ABL   Atmospheric boundary layer
ASET   Available safe evacuation time
CAARC Commonwealth Advisory Aeronautical Research Council (standardised test building)
CFD   Computational fluid dynamics
CFL   Courant–Friedrichs–Lewy (condition)
CUBE Silsoe cube building
CWE   Computational wind engineering

* Correspondence should be addressed to: Wojciech Węgrzyński, E-mail: w.wegrzynski@itb.pl

DES   Detached eddy simulation
DNS   Direct numerical simulation
DSM   Differential stress model
EVM   Eddy viscosity model
FDS   Fire dynamics simulator
FSE   Fire safety engineering
FSI   Fluid–structure interaction
LES   Large eddy simulation
MEM   Mesoscale meteorological model (also MMM)
MIM   Microscale meteorological model
NIST   National Institute of Standards and Technology (Gaithersburg, USA)
NSHEV   Natural smoke and heat exhaust ventilation
RANS   Reynold's averaged Navier–Stokes (equations)
RSET   Required safe evacuation time
RSM   Reynold's stress method
SAS   Scale adaptive simulation
TTB   Texas Tech Building
URANS   Unsteady RANS
WUI   Wildland–urban interface

1. Introduction

1.1. Scope of the Paper

Wind and fire together can form a devastating force of nature. Most of the known fire phenomena will change their behaviour when subjected to wind and, in most cases, this change will be to the worse. With wind, the fire spread rate is faster, smoke moves further, and unexpected change in the internal flow may be deadly to exposed parties or firefighters [1]. With such a profound impact on fire behaviour, it is surprising that the advances of computational wind engineering (CWE) [2] are so rarely used in fire safety engineering (FSE).

This paper forms Part II of the work dedicated to the coupling of fire safety engineering and computational wind engineering. Part 1 covered a literature review of the many instances of wind and fire coupled analyses, related to full-scale measurements, wind tunnel tests and the mathematical or numerical CFD modelling of phenomena. The research was subdivided into six categories: (1) wind and fire interaction; (2) indoor flows and natural smoke control; (3) natural smoke ventilator design; (4) tunnel ventilation; (5) wildfires and firebrand transport; (6) smoke dispersion in urban environments. Most of the research described in Part I did not fully follow the good practice guidelines used by CWE. Thus, it was evident that the transfer of knowledge between these two disciplines was necessary, and could bring benefits to both fire and wind engineers.

The primary goal of this review paper is to transfer some of the best guidelines of CWE into FSE-related CFD modelling. The area that may benefit the most, from this diffusion of knowledge, is the modelling of natural smoke ventilation of buildings and tunnels. The findings and recommendations of this work may also be useful for modelling wildfires, urban-scale smoke dispersion or large smoke plumes. This paper does not cover the subject of modelling wind along with fire entirely. In fact, the application of numerical modelling to this combination of

phenomena can be still considered as a young field of study, requiring more validation from wind tunnels and large-scale experiments.

1.2. *Common Areas of Wind and Fire Modelling in CFD*

Difficulties in modelling wind arise from the necessity to capture three-dimensional flow features such as vortex creation, shedding, flow detachment and reattachment from and to surfaces, and the whole area behind the structure, along with resolving the pressure field on the surfaces which are boundaries to the flow. It is also necessary to define if the user is interested in mean values only or also in peak values induced by wind gusts. Wind engineering may focus on these problems; however, in some cases, they may be irrelevant to fire engineering. In order to transfer successfully the best practice guidelines from CWE to FSE, it is necessary to find the common fields between the disciplines, especially in the areas of: (a) turbulence modelling and time discretisation; (b) spatial discretisation, the size of the domain and the size of the grid; (c) introduction of the wind characteristics as boundary conditions.

The scale of the analysis and modelled flow velocities will be different in FSE and CWE simulations. This leads to significant differences in the use of turbulent flow sub-models. In CWE, the RANS modelling in the steady-state simulation is still the most common approach, despite the fact that URANS (transient, unsteady RANS) and LES modelling can provide more realistic results. There is no single best-choice turbulent flow sub-model in wind engineering, as different types of analyses will focus on different phenomena. It is widely accepted that RANS produces sufficiently accurate results at a low computational cost [3]. In FSE, the prevalent approach for turbulence modelling is LES.

A major difference between use of CFD in FSE and CWE lies in the size of numerical domains used for the studies. In the case of fire modelling, it is usually sufficient to model the interior of a building or its nearest surroundings. In wind engineering, the size of the domain must be sufficient to resolve the flow to the front and behind the building but also in a lateral direction and over the building of interest, in a way that assures that the domain does not affect the flow itself [4].

The introduction of the wind into the numerical model can also be a challenging task. In addition to the choice of wind velocity and the description of its turbulence—based either on historical data, real time measurements or meteorological models, it is essential to define a mathematical description of the vertical profiles of these parameters in the function of the domain height. In many cases, the domain must be also built in a way, that allows forming of proper wind boundary layer, which is a good representation of natural phenomena.

2. Guidance Documents for Computational Wind Engineering

2.1. *Good Practice Guidelines for Computational Wind Engineering*

Referring to wind and fire coupled CFD analyses, to the best of the authors' knowledge, there was no single guidance document that dealt with both phenomena. The best practice guidelines for the whole discipline of computational wind

engineering are summarised in a thorough review paper by Blocken [2]. Among the documents listed, the ones dedicated to urban physics and natural ventilation modelling can be considered the closest to wind-fire coupling. Thus, the reader is also redirected to another review published by Blocken [5], in which the CFD use in urban physics is thoroughly described. The author proposed 'ten tips and tricks towards accurate and reliable CFD simulations', out of which many are incorporated in the recommendations given in following sections. The next useful guideline document with particular recommendations is provided by Ramponi and Blocken [4]. In this paper, the authors present guidelines towards modelling the natural ventilation (cross-ventilation) of buildings, with an interesting discussion of the importance of various user-defined parameters on the results of the analysis. Besides the above-mentioned works, many good practice guidelines are available for CWE [3, 4, 6–16]. This list is not exhaustive, and the reader is advised to seek the guidelines relevant to his/her research topic in the summary paper [2].

In addition to guidelines, this paper also covers essential research on the flow over flat roofs and to the flow around a single building. The most basic issues are considered, but they are relatively well described in relation to full-scale and model-scale measurements, as well as numerical simulations. They also illustrate difficulties which can be encountered during wind action analyses and provide a large database of information to employ in coupled analyses.

One of the essential CWE guidelines was described by Franke et al. [3, 7, 8] as the result of European Cooperation in Science and Technology (COST) actions. The presented recommendations are appropriate mainly for the prediction of mean velocities and turbulence intensities in urban areas and cover a quite large field of applications. They are related mainly to steady RANS but also to URANS, LES and hybrid models.

Other widely documented guidelines are provided by the Architectural Institute of Japan (AIJ) within a project whose aim was to elaborate recommendations for CFD use in the design process (the most important papers are: [6, 9–11]). In several papers, the flow around (1) an isolated building in the boundary layer (*L*: *W*: *H* = 1:1:2 and 4:1:4), (2) a simple city block, (3) a high-rise building in the city, and (4) a complex of high-rise buildings was computed with the use of different RANS and LES models.

Recently, the most extensive review of LES applications in wind engineering, primarily related to the simulation of the boundary layer, wind action on structures, flow over the terrain of complicated orography, wind climate in urban terrain and finally pollutant dispersion, was published by Tamura [12] within the working group of the AIJ. He argued that LES is better than RANS for the evaluation of peak values of wind gusts and, consequently, peak loads. He also pointed out that there is a necessity to make simulations, which would be validated by in situ measurements. This would lead to the establishment of simulations independent from wind tunnel tests in the future. This statement was verified by practice over the past decade, and it is important to note that in the field of wind engineering the majority of CFD results are still validated by wind tunnel and in situ tests. Blocken et al. [13] used best guidelines performing simulations on pedestrians' wind comfort in a campus at Eindhoven University of Technology.

The results obtained with the use of Realizable k–ε were validated by in situ measurements, which allowed the improvement of current recommendations.

Tominaga and Blocken [14, 15] compiled a broad set of data on flow and dispersion in cross-ventilated buildings. Wind tunnel studies were performed in a simple building in a scale of 1:100 and dimensions of 0.2 m × 0.2 m × 0.16 m with various locations of ventilation openings. The measurements were conducted for CFD validation purposes and, consequently, for the future elaboration of guidelines for such flow and dispersion issues. The validation of several RANS (k–ε standard, RNG k–ε, Realizable k–ε, k–ω, RSM) and LES simulations of cross-ventilation in a generic-shaped isolated building was carried out in a paper by van Hooff et al. [16]. The results of the computations were related, among others, to the mean flow velocity, turbulent kinetic energy and ventilation flow rate. It was shown that LES better reproduced all these parameters and it was concluded that the choice between different models should be based on the desired target value.

2.2. *Research on Wind Action on Flat Roofs*

When considering smoke control systems in buildings, it is suitable to utilise data obtained in numerical simulations, models or in situ measurements designated for wind action on civil engineering structures. It is well known that not only perpendicular but also oblique angles of wind attack on the roof should be considered. Oblique wind action can induce conical vortices over the roof, which produce large suction at areas close to its windward edge. Such an increase of suction should be taken into account while designing ventilators, and their spatial arrangement on the roof. According to the authors' knowledge, there are many papers which provide data related to pressure and velocity fields on and over roofs, which could also be used in coupled wind and fire analyses. Some of the most valuable, in our opinion, related to flat roofs and are, thus, in their most basic form, suitable also for validation purposes of CFD. These are listed below.

The measurements of wind action on flat roofs are mainly focused on wind pressure and velocity fields over them. The results are related to: low-rise buildings of a circular cross-section (wind tunnel—Uematsu et al. [17, 18]), buildings of square or rectangular cross-sections (full-scale—Richards and Hoxey [19, 20], wind tunnel—Gerhardt and Kramer [21], Lipecki [22]), flat roofs with and without parapets, attics or other edge barriers (full-scale and wind tunnel—Stathopoulos et al. [23], wind tunnel—Kareem and Lu [24], Pindado and Meseguer [25]), use of Wall of Wind (WoW) for models in a scale 1:10 (full-scale or large scale 1:2—Blessing et al. [26], Mooneghi et al. [27]), multi-level roofs (wind tunnel—Cao et al. [28, 29]) or interference effect of neighbouring buildings (wind tunnel—Pindado et al. [30]).

Angles of wind attack perpendicular to the edges of the roof were considered in full-scale tests on a Silsoe Cube in the above-mentioned papers [19, 20]. Many types of research have focused on oblique angles to discover conical vortices over the roof (full scale—Wu et al. [31], wind tunnel—Tieleman et al. [32, 33], Kawai [34], full-scale and wind tunnel—Banks et al. [35]).

When discussing CFD simulations of flow or pressure over and on the roof, the paper by Stathopoulos and Zhou [36] published in the relatively early stages of CWE development must be mentioned. Their aim was to calculate pressure on the roofs of buildings of different heights with the use of RANS models. LES simulations were described by Ono et al. [37], who represented roof pressure caused by conical vortices which appear at oblique angles of wind attack.

All of these above-listed works are documented in detail and provide valuable information and a broad set of data related to wind velocity and pressure fields which can be used to validate CFD simulations, as well as to incorporate them into guidelines for CFD simulations of fire–wind coupled actions. Moreover, the results of numerous measurements and simulations common in CWE and related to roofs of different shapes, like mono- and duo-pitch, hipped, multispan, vaulted etc., can also be considered in wind-fire analyses.

2.3. Research on Flow Around an Isolated Building

The vast range of data is provided by numerical simulations and measurements performed on a few engineering structures in full-scale or scaled-down models. In the field of wind engineering, the following structures have been used throughout the years to validate various theoretical and numerical models of flow around a single building: the Silsoe Cube, the CAARC (Commonwealth Advisory Aeronautical Research Council) building and TTB (Texas Tech Building). Below, very well-documented experiments and simulations performed for these buildings are briefly specified. The experiments are related to issues of importance also for fire engineers, like flow fields around objects or pressure distributions on their surface.

As already mentioned, Richards and Hoxey [19, 20] described the flow around the flat roof of the Silsoe Cube (6 m × 6 m × 6 m). Various aspects of the flow field around the Cube and the pressure coefficients on it were raised in [38] and compared with available data from the literature. Wind velocities and directions together with pressure measurements on the side walls of the Cube were presented in [39]. The primary aim of these tests was to define the reattachment of the boundary layer to the surface of the object. A comparison of pressure characteristics between the model and full-scale tests were described in [40], where the reasons for observed and possible discrepancies were also clarified. The mean and extreme values of pressure coefficients on the Cube walls and their standard deviations in wind conditions, as related to open terrain flow for different angles of wind attack, were described in [41, 42]. Over the span of a decade, Richards and Hoxey performed very detailed experiments on the different aspects of flow behaviour around the Cube, making it one of the most precisely measured structures in aerodynamics. Throughout the years, the data was used for CFD validation as well as for checking the correctness of tunnel experiments. Other notable research on the CFD modelling of pressure on the Cube's surface was presented in [43, 44]. In this research authors compared some of the best-known RANS turbulence models (k–ε standard, MMK k–ε, RNG k–ε, DSM), and more complicated two-layer models with non-linear ones and with each other. It was pointed out that all models gave bigger or smaller differences when compared to the field measure-

ments. More recently, Richards and Norris [45] simulated, using LES, the unsteady flow over the Cube in case of perpendicular wind action on its façade. Pressure changes on the roof and side wall reproduced correctly full-scale observations. Other recent analyses [46, 47] were related to LES simulations of wind velocities, façade pressures and ventilation rates, and to measurements comparisons.

Another structure essential to wind engineering is the CAARC building. In contrast to the Cube, this is a high-rise building of the following dimensions: cross-section of 45.72 m × 30.48 m and height of 182.88 m. Melbourne [48] performed model tests on the pressure on the walls of the CAARC building in six wind tunnels and got the scatter of results within 15%, but did not determine any distinct dependence on wind flow parameters. Goliger and Milford [49] checked the influence of the geometry scale of the model (low influence) and the profile of the longitudinal turbulence (relatively higher influence) on the response of the CAARC building. Another wind tunnel study was performed on two identical models of the CAARC building placed one by one in order to investigate aerodynamic interference [50]. Various RANS and LES simulations validated by measurements performed in seven wind tunnels were described by Huang et al. [51], who compared the mean and RMS values of pressure coefficients on walls and wind velocities around the building. Satisfactory results were obtained with the RANS simulations, especially with the use of the MMK k–ε turbulence model. The RANS model coupled with the so-called "kinematic simulation" allowing simplified simulation of wind field characteristics was described in [52]. The influence of turbulence intensity and length scale on the behaviour of the CAARC building was examined in [53] with the use of LES and the so-called "inflow generator" allowing for the introduction of turbulence characteristics at the domain inlet. Another approach to generate inflow boundary conditions was applied in LES simulations performed on an isolated and surrounded CAARC building in [54]. The aerodynamic behaviour of the building was validated by wind tunnel studies. One of the first papers about FSI (Fluid–Structure Interaction) in wind engineering, using LES and FEM coupling, was published by Braun and Awruch [55]. The authors represented quite well the aerodynamic behaviour of the CAARC building, which was proved by comparison to wind tunnel tests and other simulations.

Finally, the third building described in detail in wind engineering is TTB, with cross-section dimensions of 13.7 m × 9.1 m and a height of 4.0 m. Pressure on TTB walls and wind field data archived at near-standing mast were described by Levitan and Mehta [56, 57]. Practically all later experiments and simulations were related to these data. Wind tunnel tests on the scaled-down TTB were described in several papers [58–61], where the influence of geometric scale, inflow turbulence etc. was examined. Some experiments on pressure distribution on the TTB roof were mentioned above [31–33]. Different analyses of roof pressures on this building were also described in [62–64].

In the early stages of CFD development in wind engineering, Selvam got quite satisfactory results of surface pressure and wind velocities over TTB in simulations using the RANS models (k–ε standard and KL k–ε) [65] and LES [66]. Stathopoulos [67] summarised the early achievements of CFD in wind engineering.

Besides TTB, he also considered the Cube and buildings of other shapes. Statho-poulos pointed out that the spread of the results of simulations was more or less similar to the discrepancies obtained in various experiments and, in general, was at an acceptable level. The windward edges of the roof and side walls, where detachment takes place, were the exceptions, and suction was overestimated in these places. This problem, mainly encountered in RANS simulations, is still relevant nowadays. A couple of years later, additional CFD simulations (various k–ε models) were presented in [68], where the authors applied a three-stage procedure allowing the determination of wind field characteristics, the simulation of turbulent wind fields and the pressure on building surfaces.

3. Recommendations for Spatial and Temporal Discretisation

3.1. *Size of the Domain and the Level of Detail*

Many rules of CWE originate from decades of testing in wind tunnels. One such rule is that the blockage ratio in the cross-section at which flow occurs should not be larger than 3% [3]. The blockage ratio can be described as the proportion of the cross-section of the building to the cross-section of the domain, in a plane perpendicular to the flow, Fig. 1. In the urban flow analysis, it may be necessary to include a few rows of surrounding buildings in the model, which may influence the flow around the building of interest. In some cases, when the terrain rough-
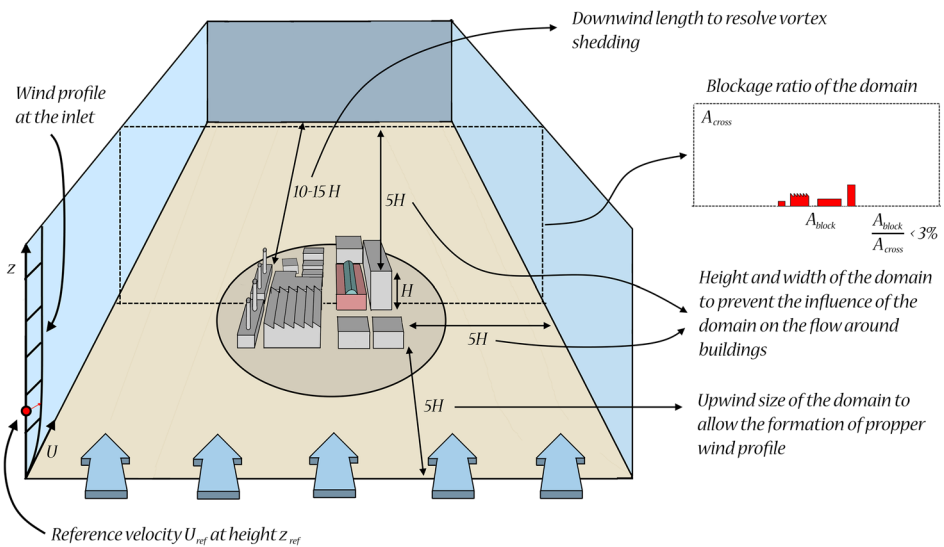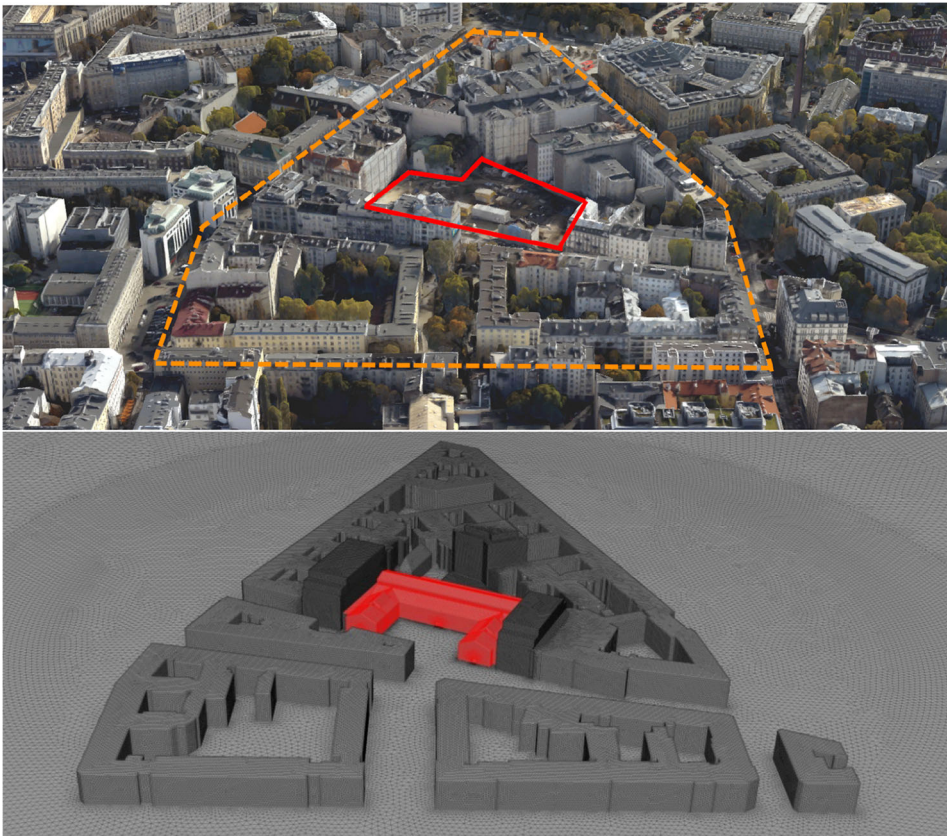

Figure 1.   Illustration of the numerical domain and its dimensions recommended for wind and fire coupling analysis. *H* is the height of the highest explicitly modelled building.

ness is included in the numerical model, and proper wind modelling function is used at the inlet boundary, it may be sufficient to include only the buildings in the closest proximity to the one tested. Nevertheless, a sensitivity analysis regarding the size of the domain should be performed. An example of the level of detail of surrounding buildings included in the numerical domain for the coupled wind and natural smoke control CFD analysis is shown in Fig. 2.

The inlet has a lateral and top boundary which should be at least $5H_{max}$ away from the group of explicitly modelled buildings, and H_{max} signifies the height of the tallest building. The reason for this is to limit the error caused by the modelling of the airflow velocity in the building proximity—too small a domain will cause strong artificial acceleration or blockage of the flow (Fig. 3). As the dynamic pressure of the airflow determines the performance of NSHEVs, this error is significant for the natural ventilation performance assessment [69]. The

Figure 2. Aerial photograph of Warsaw (upper picture, *source*: Google Earth) and the numerical domain in the model for the investigation of smoke control in the middle building (bottom picture) [146].
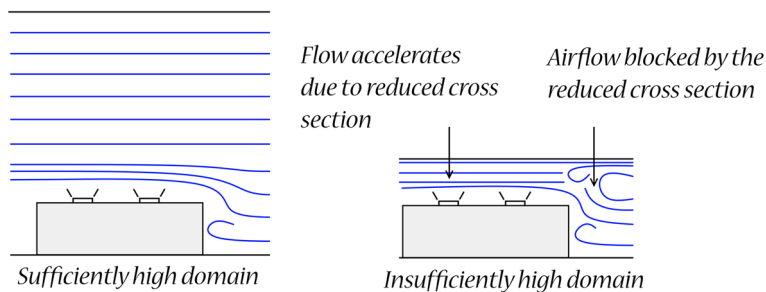
Figure 3. Effect of the insufficiently high domain on flow above the roof of the building.

outflow boundary should be at least 10 [6] to 15 [7] H_{max} away from the group of explicitly modelled buildings, to allow development of the full wake flow, which is crucial if inlets to the building are placed on the leeward side of it. A detailed discussion of the influence of the domain size on the results of numerical analysis is presented by Ramponi and Blocken [4]. In their analysis of the natural ventilation of buildings, they observed a significant error connected to the reduction of the domain dimensions (increase of the blockage ratio).

The set of recommendations elaborated by the COST and AIJ groups is collected in Table 1, whereas a few examples assuming computational domain and grid resolution for well-documented investigations are shown in Table 2.

When considering flow, dispersion, smoke etc. in urban terrain, it is necessary to represent a broader region. It is assumed, on the basis of wind tunnel tests, that a building of a height H_b has an influence on the considered area when it is

Table 1
Relevant Guidelines for the Size of the Domain in CWE

Refs.	Height H	Width W	Upwind length L_u	Downwind length L_d	Grid
[3], [7]	$5H_b$	$5H_b$ $2.3W_b$	$5H_b$	$15H_b$	Min. 10 cells on building side Urban area—level of analyses should be at the 3rd and 4th grid level over the ground (1.5 m to 2 m)
[6]	$5H_b$	$5H_b$		$> 10H_b$	Simple building—min. 10 grids on one side to reproduce the separation flow around the windward edges Urban area—min. grid about 1/10 of the building size (0.5 m to 5 m) in the region of interest Urban area—level of analyses should be at 3rd or higher grid level from the ground (1.5 m to 5 m)

$H_b = H_{max}$—height of the highest building in case of a group of buildings in the built-up area, W_b—width of the built-up area. Distances are given from the object/group of objects to domain boundaries

Table 2
Examples of Domain and Grid Sizes in Relevant CWE Studies

Refs.	Building $W_b \times L_b \times H_b$	Domains $W \times L \times H$	Discretisation, no of grids along W, L, H	Turbulence model
[11], [110]	$1 \times 1 \times 2$, $W_b = 0.08$ m	$(11.25 \times 21.5 \times 13.75)W_b$	$45 \times 60 \times 39$ Min. grid size—$0.07W_b$	RANS LES
[13]	$H_{max} = 82.8$ m, TU/e campus	Dependence on wind attack $W = (22.2 - 27.26)$ H_{max} $L = (25.08 - 32.84)$ H_{max} $H = 10.06\ H_{max}$	Min. grid size: $0.2 \times 0.7 \times 0.18$ m Max. grid size: $70 \times 70 \times 120$ m	RANS
[94]	$1 \times 1 \times 0.5$, $1 \times 1 \times 4$	$(20 \times 30 \times 10)H_b$—low-rise $(20 \times 32 \times 10)H_b$—low-rise $(18 \times 22 \times 10)H_b$—low-rise $(5.4 \times 9 \times 10)H_b$—high-rise	Grid size next to building surface $< W/100$	RANS LES
[55]	CAARC, full scale $1 \times 0.67 \times 4$ $W_b = 45$ m	$(4.7 \times 10.17 \times 4.5)H_b$	–	For FSI purposes
[51]	CAARC, 1:250	$(4.25 \times 7.17 \times 2)H_b$	On building surface—height of the first boundary layer—$W_b/4000$	RANS, LES
[54]	CAARC, 1:400	$(18 \times 30 \times 5)H_b$	Max. grid on building $H_b/70$	LES
[53]	CAARC, 1:400	$(10 \times 20 \times 4)H_b$ $(8 \times 10 \times 4)H_b$	–	LES
[45]	CUBE, full scale $W_b = L_b = H_b = 6$ m	$(10 \times 15 \times 6.67)H_b$	$123 \times 246 \times 186$ Min. size: 0.02 m, max. size 0.5 m	LES

W_b, L_b, H_b—width, length (depth), height of the building respectively, W, L, H—width, length, height of the domain respectively

within $6H_b$ from the area. In this case, the building should be included in the model [3, 7].

It is also worth mentioning the paper by Revuz et al. [70], in which a revision of the guidelines for building the computational domain for the flow simulation around high-rise buildings is presented. The authors focused on the domain size leaving the grid in the wake region of the building unchanged. On the basis of parametric computations, they found that the domain of a volume of 10% the recommended one introduces loss with an accuracy of less than 10%. Of course, these findings cannot be generalised, and in every case study a domain sensitivity analysis should be performed.

The main difficulty of applying wind and fire coupling in building-related simulations, comes from the requirement for a high-quality representation of the roof

and its details in the analysis—resulting in massive scale differences between the smallest and largest elements in the model. According to the experience of the authors, for models of natural vents, details larger than 5 cm should be represented in the ventilator model. These elements can influence the discharge coefficient C_v of the ventilator by more than 0.02. Samples of detailed models of ventilators are shown in Fig. 4.

## 3.2. Quality of Space Discretisation

Following Blocken [5], a fine numerical mesh may be characterised by its: (1) overall grid resolution, (2) quality of computational cells regarding shape (including skewness), orientation and stretching ratio. In general, many of fire-oriented CFD studies use coarse structured meshes and, only rarely, any form of boundary layer mesh. Some examples of grid discretisation in CWE are summarised in Table 2.

In some CFD models used for wind and fire coupled analysis (e.g. ANSYS Fluent, STAR CCM +, OpenFOAM) it is possible the use unstructured meshes (the definition of structured and unstructured meshes and shapes of elements is presented in Fig. 5), and such function is also under development for FDS (in form of immersed boundary method [71, 72]). Albeit unstructured meshes allow easier mesh generation, especially for complex geometries, their use may lead to problems with the convergence of the simulation. A solution to this is the general improvement of mesh quality (examples of high-quality tetrahedron meshes are presented in Fig. 4, examples of high-quality unstructured prism meshes are given in [5]).

The choice of individual cell dimensions is not a trivial problem. Among many length scales that should be considered when determining grid resolution, a non-dimensional expression $D^*/\delta x$ is especially popular for simulations involving buoyant, thermal plumes. Thus, the use of $D^*/\delta x$ expression as the indicator of the validity of the numerical mesh has become the main approach in many of
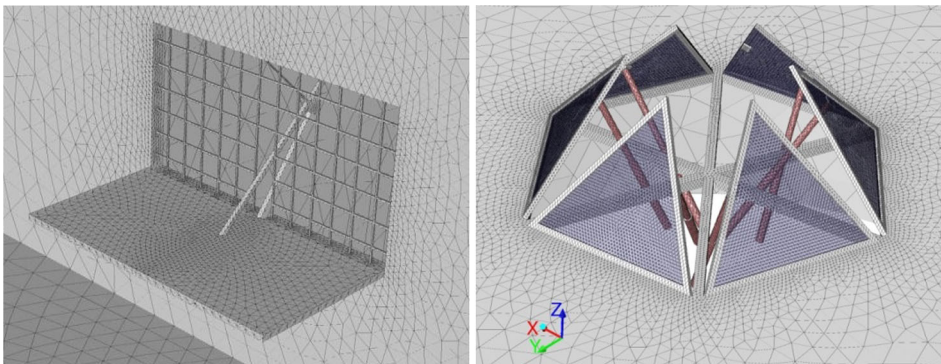
Figure 4. Examples of numerical models of complex natural ventilators used in the estimation of C_v (own unpublished work).
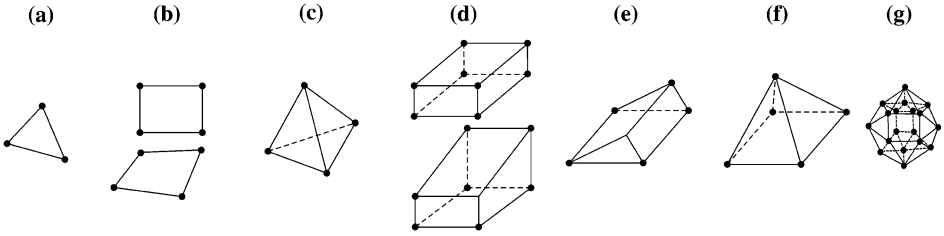
Figure 5. Elements used in CFD, 2D: (a) triangles, (b) quadrilaterals, 3D: (c) tetrahedrons, (d) hexahedrons (bricks), (e) prisms (wedges), (f) pyramids, (g) polyhedrons. Structured meshes—regular shapes (b) and (d), unstructured meshes—irregular shapes.

FSE-oriented CFD simulation. D^* is the characteristic fire diameter, which can be calculated according to Eq. 1, and δx is the size of a mesh cell [73]. A review of the use of $D^*/\delta x$ is given in [74]. This is not the sole length scale that may be of importance, especially if the user aims to resolve the flows through small openings (e.g. leakages) or around minuscule details of natural vents (e.g. wind baffles, traverse, motor). Also, no matter the approach used to choose the length scale, a recommended approach is to always perform a mesh sensitivity study.

$$D^* = \left(\frac{\dot{Q}}{\rho_{amb} c_p T_{amb} \sqrt{g}} \right)^{2/5} \tag{1}$$

where $\dot{Q}$ the heat release rate of fire (kW), ρ_{amb} the density of ambient air (kg/m^3), T_{amb} ambient temperature (K), g constant of gravity (N/kg), c_p specific heat (J/kg).

A wide range of validation cases for the FDS solver (LES approach) is presented in Table 3.13 of [75]. As a rule of thumb it may be said, that in most FSE-oriented studies, the grid size sufficient for the solution of the fire problem is between 10 cm and 20 cm. To meet general recommendations for the flows around a building model, at least 10 cells per cube root of the building volume, and at least ten cells between buildings should be used. In the ground layer, at least five elements should be placed at the height at which velocity is critical—a rule that may be extended to both pedestrian level inlets to the building and roof level outlets. Again, even if the user meets these recommendation, the user is expected to perform a mesh sensitivity study, through which s/he can prove that further improvement of the mesh did not affect the quantitative results of the simulations.

The quality of the mesh used in the analysis may be investigated through a posteriori mesh quality metrics, as described in [73]. The most popular of these metrics is a scalar quantity named 'measure of turbulence resolution', coined by Pope [76]. It is generally expected that the turbulence model (LES in this case) resolves at least 80% of the kinetic energy in the flow. Another method to verify the quality of the mesh and the grid independence of measured parameters is the method

proposed by Roache [77, 78]—the Grid Independence Index. An example of the practical use of this method is shown in Blocken [5].

In order to resolve accurately the flow near a wall, a sub-model called wall function has to be used, upon which depends the mesh resolution at the wall boundary. A standard way to measure the near-wall resolution is through a non-dimensional distance from the wall—y^+—which can be calculated with Eqs. 2 and 3.

$$y^+ = \frac{u_* y}{v} \tag{2}$$

$$u_* = \sqrt{\frac{\tau_w}{\rho}} \tag{3}$$

where y^+ non-dimensional wall distance (m); u_* friction velocity (m/s), v kinematic viscosity of the fluid (m/s^2), τ_w wall shear stress (Pa), ρ fluid density at the wall (kg/m^3).

The required value of y^+ depends on the type of turbulence model and type of wall function sub-model used. In the case of FDS, which employs the log-law model, the expected values of y^+ should be between 30 and 100. A similar good practice guideline may be followed for RANS simulations with wall functions.

The second essential mesh requirement—the quality of the computational cells regarding their shape—is explicitly met if a Cartesian structured mesh is used. For unstructured meshes, this should be a part of the individual analysis. Unstructured meshes may increase truncation errors and cause issues with convergence. Conversely, the user may encounter difficulties with the Cartesian mesh in terms of its orientation and the growth rate factor. Orientation plays a significant role during the oblique angle sensitivity study of the approaching flow, which should include 12 different wind velocity angles [8]. With the Cartesian mesh it may be difficult to rotate the model, without introducing additional errors.

A recommended growth ratio of elements should not exceed 1.30:1 [7], while for the Cartesian mesh it should not exceed 2:1 [73]. A mesh sensitivity study should be performed to assess its influence on the flow. A relevant guide on high-level mesh generation for a coupled outdoor and indoor analysis was presented by van Hoof and Blocken [79].

3.3. Time Discretisation

As previously mentioned, the typical CWE analyses are performed as steady-state solutions. It is assumed that the steady-state solution represents the flow characteristics in a given volume as independent of time. Considering the problem from a wind engineering point of view, the use of steady or unsteady simulations depends on the desired results which one would like to obtain. When a study is focused on the flow behind the building, then both steady and unsteady RANS simulations could be burdened with significant inaccuracies. Conversely, the use of LES to get the exact time-dependent flow behaviour increases the time of compu-

tations, the necessary computer power and, in consequence, the overall costs. In any case, the user must strike a balance between acceptable accuracy and costs.

In FSE, most of the analysis is carried out as unsteady (transient), as the fire itself is a transient phenomenon. Thermal effects, which are neglected in wind-related analyses, have a strong influence on the solution in fire-related analyses (plume flows, ceiling jets, pressure differences etc.).

Performing all wind and fire-related studies as transient would require immense computational power, a simplified solution is to use the two-step approach presented further in the paper. First, multiple steady-state analyses may be performed to find the worst-case scenarios for wind (based on the values of pressure coefficients), and then these cases are verified with the transient analysis in fire conditions.

An important aspect of unsteady modelling is the correct choice of the discrete time step. In some cases, such as in the FDS solver, the time step length is evaluated automatically by the solver, based on the CFL (Courant–Friedrichs–Lewy) criterion, which is mostly dependent on the size of the numerical mesh and the flow field [80]. In the case of other solvers, especially ones that use URANS modelling, different lengths of time steps may be adequate for different phenomena investigated. As a rule of thumb, implicit upwind schemes are preferred, and the solver should provide proof of convergence. If, however, the default convergence criteria are too loose, oscillatory convergence behaviour may be observed [5].

4. Turbulence Modelling

For detailed information on the turbulence models used in CWE, the reasoning behind the choice of the most appropriate model and their validation, please refer to e.g. [2, 81–83]. As mentioned in [84], however, 'the relevance of turbulence modelling only becomes significant in CFD simulation when other sources of error […] have been removed or properly controlled'.

For applications in wind engineering, the typical turbulence models are:

- Steady Reynolds-averaged Navier–Stokes (RANS);
- Unsteady Reynolds-averaged Navier–Stokes (URANS);
- Large Eddy Simulation (LES);
- Hybrid URANS/LES approach (e.g. DES).

Throughout the years, many different models were implemented, with varying degrees of success, in wind engineering issues. The basic group—EVM (Eddy Viscosity Models)—is based on the assumption that Reynolds stresses are proportional to the strain rate. There is a large group of two-equation RANS models based on the eddy viscosity assumption, the most popular of which is the k–ε standard [85]. The main disadvantage of this model is an overproduction of turbulent kinetic energy, k, at windward surfaces at flow stagnation point. The k–ε standard model was modified into new models, to improve the flow in the front of the building as well as in the wake region in relation to wind velocities. Among

multiple others, we find: RNG k–ε [86], Realizable k–ε—RLZ k–ε [87]. Another way of closure for RANS equations is assumed by the k–ω model, where the turbulent dissipation, ε, is replaced by the specific dissipation, ω [88]. The most often used model of this family is k–ω SST [89]. Years of use of common RANS models in wind engineering revealed their weaknesses in the proper modelling of the flow around objects, especially with sharp edges. The RANS models family consists of multiple models, while the best fit for CWE applications was shown to be Realizable k–ε and RNG (Renormalisation Group) k–ε [3]. The standard k–ε model is not recommended for this application.

Another group of models is the Reynolds Stress Models (RSM). The Eddy viscosity hypothesis is not used here, and exact Reynolds stress transport equations are used for the formulation of particular components of the Reynolds stress tensor. There are several variants based on the different solution for the pressure-strain relation, which can be described by linear, quadratic or cubic equations. In general, the simulations are considerably longer compared to EVM models and are used in wind engineering sporadically.

An entirely different approach is used in Large Eddy Simulation (LES) models. LES was elaborated by Smagorinsky [90], who proposed the simulation of large vortices with the use of spatial averaging of the flow. There were multiple modifications to the model, one of the most important being made by Germano et al. [91]. In this model, large eddies in the flow are resolved directly through N–S equations, while small eddies are modelled through the sub-grid scale (SGS) model. The assumption is that small eddies are less dependent on geometry, tend to be more isotropic, and thus may be simulated in a universal way. The large eddies are usually case-dependent and since they cannot be modelled universally, they are resolved directly. The boundary between large and small eddies is referred to as the Smagorinsky filter. In the case of many of the commonly used CFD software (e.g. FDS, ANSYS Fluent), the size of the filter is the geometric mean of the cell dimensions ($(\delta x \ \delta y \ \delta z)^{1/3}$). In the most popular fire oriented code FDS, the LES model is available in multiple variants (Deardorff, Vreman, dynamic Smagorinsky, constant Smagorinsky). A comparison between these approaches, in a case study with a backward facing step, was performed by Sarwar et al. [92]. In this study, the constant Smagorinsky model performed the best, however since the publication of that paper, multiple improvements were done to the turbulence models in FDS. A paper by Toms [93] investigated the reattachment of flow with a backward facing step, for Daerdorff and dynamic Smagorinsky models, and obtained results were within 10% of experiment, for mesh with resolution of 10 cells on the step height. The user should refer to the FDS user guide [73] for reference on the newest models used in the software, and be aware, that with use of older models such as constant Smagorinsky, he/she is responsible for model validation for the fire simulations. More information on the validation of FDS LES models in the case of the backwards-facing step can be found in [75].

LES can be considered superior in terms of physical modelling when compared to the RANS and URANS approaches. As described by Blocken [5], it is suitable for simulating three specific characteristics of the turbulent bluff body in urban physics: the three-dimensionality of the flow, the unsteadiness of large-scale

flow structures and the anisotropy of turbulent scalar fluxes. The costs connected with LES modelling are significant because the method requires much higher spatial and temporal resolution; thus, it is not often chosen due to economic reasons. 3D-steady RANS simulation remains the main CFD approach in CWE and has a satisfactory degree of success in wind engineering.

Various turbulence models were compared in the previously mentioned AIJ guidelines [6, 9–11], and the validation of computations based on in situ measurements and wind tunnel tests was performed. The main differences in the results obtained in different simulations were observed in regions, which were close to the edges of the objects. It was confirmed that the k–ε standard cannot represent detachment and the recirculation flow on a building roof correctly. A similar problem appears to a lesser degree close to the base of the building. Modified k–ε models manage this problem quite well and overcome these difficulties but, conversely, overestimate the reattachment length behind the building. Simulations with LES resulted in the best projection of the flow features behind the object and made the reproduction of a periodic vortex shedding possible.

The paper by Tamura et al. [94] contains a detailed comparison of LES and RANS (MMK k–ε, Kawamoto k–ε–φ) simulations results in reference to low-rise (length:width:height = 1:1:0.5) and high-rise (1:1:4) buildings in terms of the mean and root mean square values of aerodynamic coefficients of forces and pressure. According to the authors, in order to get the best projection of the wind load on the structure, transient calculations, like LES, should be employed. Such analyses allow the calculation of peak values. Mean or time-dependent characteristics of the flow can be captured with RANS models in cases of flows with large-scale vortices. The best application of RANS models is for steady flows and the evaluation of the mean values of flow and loads. Tamura also underlined that the standard k–ε model overestimates pressure on the windward wall due to the overproduction of turbulent energy, while the separation of the flow on the windward edge of the building roof does not appear.

An interesting approach is to combine LES and RANS into one model with massively separated flows, in which large vortices are resolved by LES, while small ones by RANS. This is often referred to as the Detached Eddy Simulation model (DES) [95] and, despite simplification, it still requires similar computational power as LES [83].

A summary of validation studies on both RANS and LES modelling can be found in [2], while many of the experiments employing different approaches to turbulence modelling were presented in Part 1 of this review.

5. Wind as a Boundary Condition in Simulations

The description of the wind boundary conditions (inlet to the model) is an implementation of the meso-scale atmospheric phenomena through an Atmospheric Boundary Layer (ABL) model into the CFD (micro-scale). This implementation usually requires the knowledge of two parameters—the upstream aerodynamic roughness length and the vertical profile for the mean velocity and turbulence

properties [5]. The issue of boundary conditions introduction to CFD domain concerns two aspects—introducing ABL according to given empirical formulas or rescaling data from meso-scale to micro-scale.

As not all buildings or natural obstacles are modelled explicitly in the domain, it is common to model the obstacles influence on the flow by use of a large scale roughness, termed aerodynamic roughness length z_0 [5]. This parameter must be distinguished from the sand-grain roughness height k_s. Blocken [5, 96] does emphasize, that the confusion of these parameters may lead to substantial simulation errors. The relationship between z_0 and k_s for several codes was presented in [96]. The fire oriented code FDS does use sand roughness in the definition of surface roughness, which in the case of this solver may be considered to be 30 times higher than the chosen value of aerodynamic roughness length z_0 [73].

The aerodynamic roughness length can be computed using the Davenport classification, as updated by Wieringa (and often referred to as the Davenport–Wieringa model) [97]. This parameter will determine the velocity profile and turbulence parameters of the flow within the domain and will essentially drive the movement of the air in the proximity of the building. In a review covering 269 papers [5], Blocken describes five spatial areas for which the aerodynamic roughness length should be specified (Fig. 6). Area 1 lies upstream the explicitly modelled buildings and outside of the computational domain. The roughness of this area will determine the shape of the inlet profile and its turbulence characteristics. Area 2 lies within the domain and upstream of the buildings. In this area, aerodynamic roughness length, based on [97] can be used to shape the flow, despite obstacles within this area not being modelled explicitly. Areas 3 and 4 usually consist of explicitly shaped obstacles, and two approaches to model this part of the domain are proposed by Blocken [5]. Area 5 lies within the computational domain, but downstream of the explicitly modelled part. For more detailed good practice
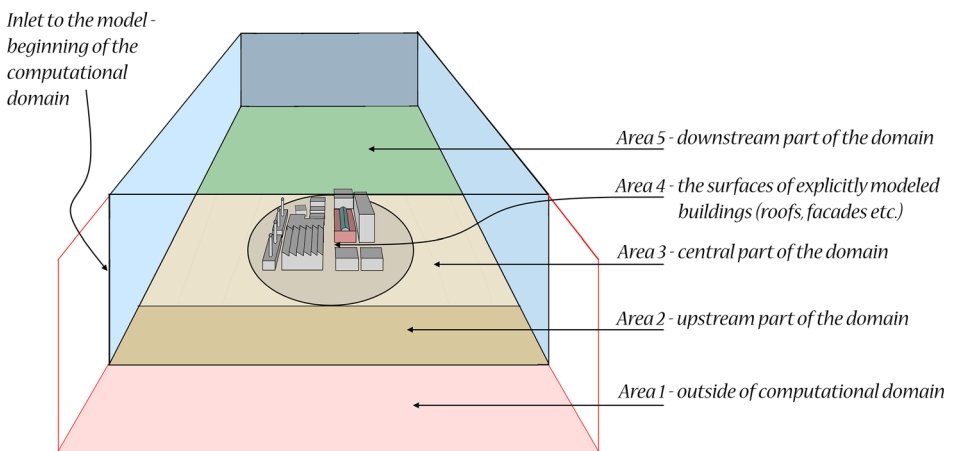
Figure 6.   Areas of the numerical domain for which roughness should be specified. Based on Blocken [5].

guidelines on shaping the domain and the choice of the appropriate terrain roughness length (or equivalent sand-grain roughness height), one should refer to the review by Blocken [5].

Introduction of the wind on the inlet boundary condition (boundary between Areas 1 and 2 is usually performed with the use of wind velocity profiles. The most commonly used wind velocity profiles in RANS simulations in the field of urban physics and wind engineering are those elaborated by Richards and Hoxey [98]. It must be noted that field measurements and reduced-scale wind tunnel measurements of turbulence intensity do not always yield a profile of turbulent kinetic energy, $k(z)$, that is constant with the height in the surface layer (assumption of the Richards and Hoxey model). An alternative way is provided by Tominaga et al. [6], who propose to obtain $k(z)$ from a wind tunnel experiment. Otherwise, a specific profile for the streamwise turbulence intensity should be provided. Both approaches, [98] with ensuing modifications and [6], are described below in detail. It is worth mentioning that despite the turbulence intensity vertical profile, turbulence length scale also influences flow especially behind the building in the wake region.

The provision of a reliable ABL modelling in LES may be ambiguous, as the turbulent behaviour of the wind cannot be simplified in the $k(z)$ and $\varepsilon(z)$ parameters, but has to be explicitly modelled in a transient approach. Some guidelines on this, related to the specific field of applications, are available in [99]. Possible solutions to the problem are: (a) synthetic turbulence generation, (b) modelling a sufficiently long inlet area of the domain for the formation of the correct turbulent layer. Approach (a) is used mainly in hybrid turbulence models as a boundary condition between RANS and LES zones [100]. A similar approach could be taken at a boundary of the domain, where the flow velocity, turbulent kinetic energy and its dissipation rate can be defined by the ABL model. A comprehensive review of possible inlet conditions for LES modelling is presented by Tabor and Baba-Ahmadi [101].

In recent release of FDS solver (version 6.6.0 dated 31.10.2017) new sub-model for wind has been introduced. The model forces mean flow velocities, and is based on Monin–Obukhov similarity parameters. This approach allows to model the velocity and temperature profiles in function of height of the domain, aerodynamic roughness length, scaling potential temperature and the Obukhov length. The default reference height for this model is 2 m, however this may be altered by the user. The description of similarity parameters is presented in [102], while thorough description of this approach is given in [73]. The mean flow velocities within the domain are driven by the FDS towards desired values by adding a forcing term to momentum equation, taking into account the relaxation time scale. This significantly eases the modelling oblique wind angles in rectangular domains. FDS solver also allows temporal and spatial variation of the wind, through ramp functions on velocity components.

Instead, or in some cases complementary to synthetic turbulence generation, it may be feasible to allow the wind to be resolved by the solver. This idea is to build a sufficiently long inlet domain, in which flow characteristics are generated through modifying sand-grain roughness of boundaries or placing blocks to tur-

bulise the stream. These obstacles will allow the formation of the turbulent boundary layer, which has to be measured and compared with the assumptions. This approach may be combined with previously mentioned sub-models, to create high quality boundary layers. Despite this approach may be time-consuming, it is usable in most of the solvers and should generally provide the best results. Regardless of whether a synthetic turbulence generator or a large inlet domain combined with block elements is used, the wind profile and the parameters of turbulent flow at the points of interest (building, fire) should be measured, and preferably validated with wind tunnel measurements.

According to Richards and Hoxey [98], ABL could be modelled as the horizontally homogeneous turbulent surface layer. This means that turbulence is homogeneous in horizontal directions parallel to the ground and varying in vertical direction, normal to the ground. The shear stress in the ABL is almost constant along the domain height and equals to values at the wall. Due to this, for calculations performed in domains much lower than the ABL upper limit, the vertical profiles of particular parameters can be simplified to the forms presented in Eqs. 4–6, where the $k(z)$ profile is constant along the height. An example of the introduction of this model as the velocity inlet boundary condition is shown in Fig. 7.

$$u(z) = \frac{u_*}{\kappa} \ln\left(\frac{z + z_0}{z_0}\right) \tag{4}$$

$$k(z) = \frac{u_*^2}{\sqrt{C_\mu}} \tag{5}$$

$$\varepsilon(z) = \frac{u_*^3}{\kappa(z + z_0)} \tag{6}$$

where z height (m), z_0 aerodynamic surface roughness length (m), κ von Karman constant (-) (0.40 to 0.42), C_μ model constant (-) (0.09), u_* friction velocity (m/s).

The formulae given by Richards and Hoxey [98] are commonly used in wind engineering calculations. The revision of the approach was elaborated several years later by Richards and Norris [103]. They extended the constant shear stress surface layer conception to provide suitable flow characteristics profiles in commonly used wind engineering turbulence models, like k–ε RNG, k–ω. The guidelines provided by COST [3, 7] and AIJ [6] also recommend the Richards and Hoxey approach. As observed, the velocity and turbulence profiles decay along the domain. Several computations were made to modify and improve the maintenance of the ABL along the fetch. The works were concentrated on the problem of how to maintain the profiles defined at the inlet to the domain almost unchanged at the outlet. Additional remarks were provided by Blocken et al. [96], who focused on wall function problems in computations of the flow in ABL over uni-
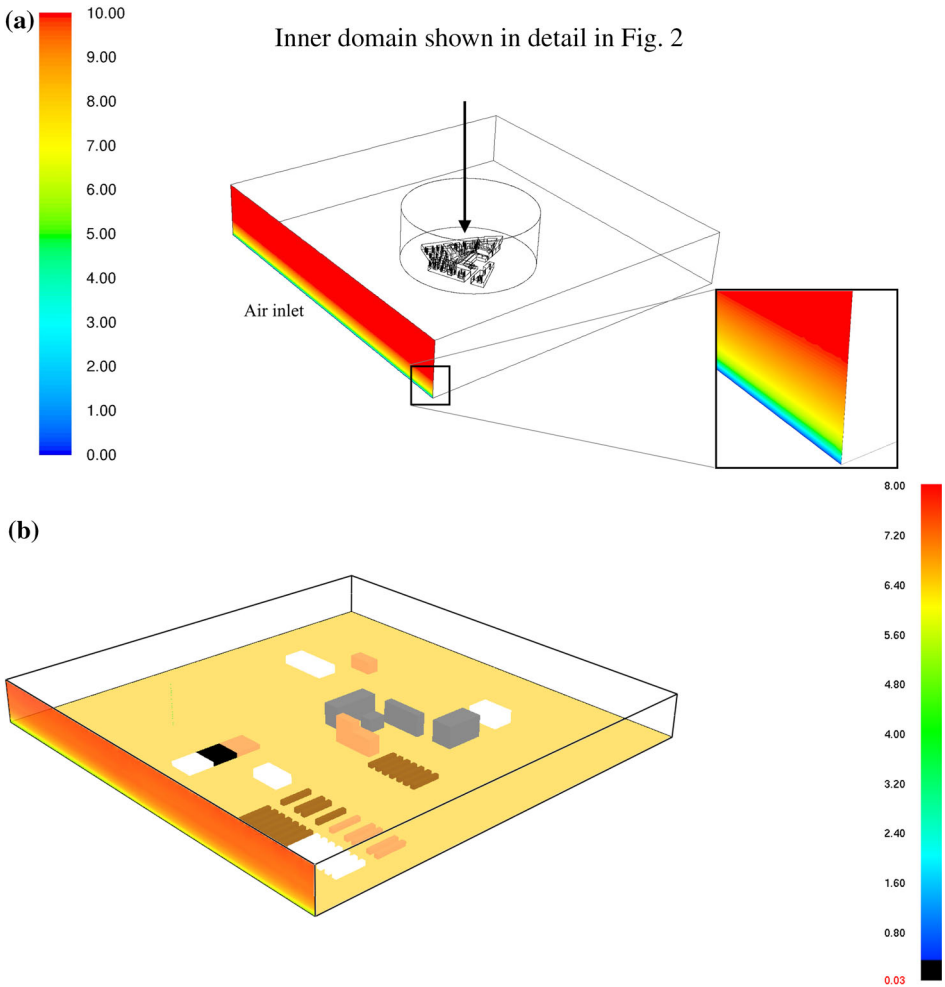
Figure 7. **(a) View of the numerical domain and the logarithmic wind profile applied at the velocity inlet boundary condition (0 m/s to 10 m/s) in ANSYS Fluent (left) [146], in numerical model used in the analysis shown in Figs. 2, 10c and 11; (b) wind introduced into numerical domain of 'wind_example.fds' example case supplied with FDS 6.6.0 with use of new WIND boundary condition [73].**

formly rough, flat terrain which is fully developed and horizontally homogeneous. Hargreaves and Wright [104] pointed out that modifications of the boundary conditions at the wall and top of the domain are necessary to reproduce ABL, described in [98], correctly along the whole fetch in the domain. Yang et al. [105] defined new turbulence boundary conditions, where $k(z)$ decreases with the height which should better represent results from a wind tunnel or full scale. Other modifications in boundary layer description were proposed in [106]. The homogeneity

of flow velocity and turbulence profiles along the domain, simulated according to the proposed procedure, was verified by computations of the flow over the flat terrain corresponding to the wind tunnel and full-scale tests and around the low-rise building placed in the ABL in the wind tunnel. Recently, another revision of their own model and its further development was presented by Richards and Norris in [107]. In this paper, computation results were compared with the theoretical model of ABL for strong winds elaborated by Deavies and Harris [108] and a quite good accordance was obtained for the lower half of ABL, where shear stresses decrease almost linearly with height.

When the wind tunnel data about the flow in a given case are available, the mean velocity, $u(z)$, and turbulence intensity profiles, $I_u(z)$ can be directly implemented in computations. Turbulent kinetic energy, $k(z)$, can be also obtained from wind tunnel measurements or from the approximate relation based on $u(z)$ and $I_u(z)$ [6]:

$$k(z) = (I_u(z)u(z))^2 \tag{7}$$

Moreover, it can be assumed in ABL that the production of turbulent kinetic energy $P_k(z)$ is locally equal to its dissipation $\varepsilon(z)$ and in consequence [6]:

$$\varepsilon(z) \cong P_k(z) \cong \sqrt{C_\mu k(z)} \frac{\mathrm{d}u(z)}{\mathrm{d}z} \tag{8}$$

The plots of $u(z)$, $k(z)$ and $\varepsilon(z)$ according to rules given in [98] (Eqs. 4–6) are presented in Fig. 8a, b, whereas the values of $u(z)$ and $I(z)$ obtained in wind tunnel measurements described in [109] together with values of $k(z)$ and $\varepsilon(z)$ calculated on the basis of Eqs. (7) and (8) are presented in Fig. 8c. In the first case, plots are divided into two parts illustrated for 200 m of the ABL and its zoom for the lower 20 m. The following data were used: $\kappa = 0.42$, $z_0 = 0.01$ m, similarly for the rural terrain, $C_\mu = 0.09$, $u_* = 0.42$ m/s. In the second case, the inlet boundary conditions are presented for the domain representing wind tunnel to the height of 100 cm [109]. When considering the whole wind tunnel height, the decrease of wind velocity caused by the ceiling of the tunnel should be taken into account (cf. [11, 110]).

The most common way to get information about wind action for design purposes is reference to standards and codes of practice. Every wind code defines basic wind characteristics within ABL: the averaging time of wind speed, terrain categories, the mean wind speed profile based on logarithmic or power-law formula, turbulence intensity in the longitudinal direction, longitudinal turbulence length scale and power spectral density of the wind speed. Turbulence characteristics in directions perpendicular to the mean wind speed generally are not provided by codes but the empirical relations between Cartesian components can be found in the literature. Most widely used wind standards are: Eurocode 1 [111], ASCE [112], AS-NZS [113], AIJ [114], ISO [115]. The very wide scope of experimental data and empirical formulas based on them in the field of wind engineering can be found in documents published by Engineering Sciences Data Unit (ESDU), the
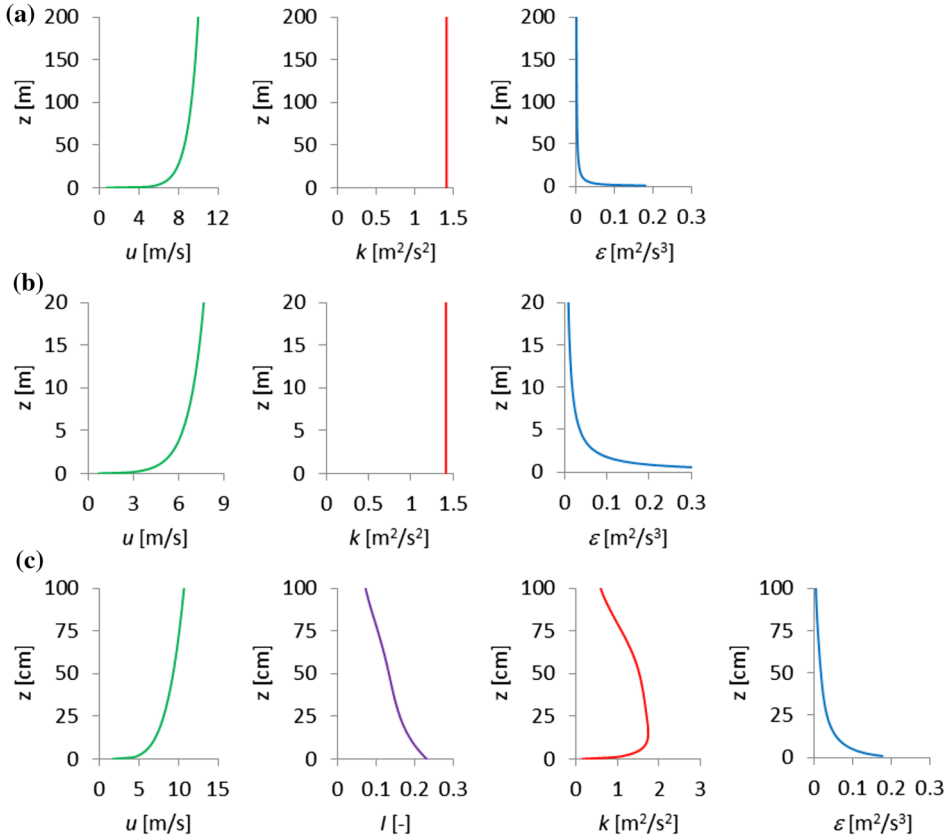
Figure 8. Wind inlet boundary conditions: (a, b) according to Richards and Hoxey [98], (c) according to wind tunnel measurements [109] and Eqs. (7) and (8).

UK engineering organization. The basic information can also be found in fundamental books for wind engineers by Dyrbye and Hansen [116], Holmes [117], Simiu and Scanlan [118], Tamura and Kareem [119].

6. Meso- and Micro-Scale Coupling Simulations

As a continuation of the previous section, here the problem of scaling wind data from the meso-scale to be used in a micro-scale is presented. One of the important points where wind engineering meets fire engineering is simulation of large phenomena like contaminant dispersion, wildfires, etc. When talking about modeling of large areas the fundamental question is: how to build the numerical domain with the satisfactory grid. It is obvious that it is not possible to take into account, simultaneously and with the same accuracy, the vertical changes of environmental

parameters within the ABL (e.g. wind, temperature, humidity, etc.) that affect the large scale phenomena (e.g. dispersion of pollutants, fire propagation, propagation of smoke clouds, etc.), the exact geometry of infrastructure in urban areas (e.g. street canyons, engineering structures) or forested areas, as well as minuscule details (structure elements, vents, inlets etc.).

In the field of simulations related to wind and fire safety engineering two spatial scales have essential meaning: meso-scale and micro-scale. The first one is over 2 km, the second below 2 km in length. With the increasing computing power, the numerical combination of these two scales becomes more common and is based on the coupling of two parts—Meososcale Meterogical Model (MMM or MEM) which has many different approaches and Microscale Metorological Models (MIM realized by CFD).

The aim of MIM or CFD is to describe wind speed or pressure fields around structures, while MEM models consider mainly topographic and thermal effects on the flow. The main differences apply to the definition of boundary conditions. For meso-scale initial atmosphere conditions together with equations considering energy and water phase changes are introduced and can evolve naturally under continuous calibration based on e.g. satellite observations [120]. Many MEM models are in use, among others: A2C (Atmosphere to CFD), ARPS (Advanced Regional Prediction Systems), COAMPS (Coupled Ocean/Atmosphere Mesoscale Prediction System), Eta, FITNAH, MEMO, METRAS, NHM (Non Hydrostatic Model), RAMS (Regional Atmospheric Modeling System), MM5, WRF (Weather Research and Forecasting), MC^2 (Mesoscale Compressible Community). The last two MEM models are used most often in coupled calculations in wind engineering.

The description of methods used for parameterization effects of obstacles in meso-scale models was provided by Schlunzen et al. [121] and more recently by Hangan et al. [120]. The authors distinguished the following approaches: (1) Main land-use approach—only the main characteristics of the land (for example buildings) are considered in a grid cell. (2) Parameter averaging method—effective values of parameters of e.g. roughness, temperature, etc., are approximated by linear or higher order averaging within a grid cell. (3) Flux aggregation method (mosaic method)—each grid cell is subdivided into a limited number of homogeneous land-use types. (4) Canopy layer (single and multi). Single-layer urban canopy model considers geometry of building areas, street canyons, exponential wind profile at the canopy level and heat transfer from infrastructure. In multi-layer urban canopy models momentum, heat, moisture are calculated at several levels. Masson [122] discussed various aspects of canopy models giving some examples of their use in urban surface modeling. Detailed review of the development of urban canopy models for meso-scale climate models were recently made by Garuma [123]. Tree representation in the single-layer canopy model was presented by Ryu et al. [124] and in the multi-layer canopy model by Krayenhoff et al. [125].

Yamada and Koike [126] summarized methods which allow to couple MEM with CWE (CFD) as: (1) The method called multi-models up/downscaling (multi-models scaling)—the meso-scale model results are used as the boundary conditions for a CWE model. In general simulations are realized for two domain-

s—coarse with meso-scale model settings and fine with CFD settings. Particular application of this method composed from: WRF–RTFDDA (Real-Time Four-Dimensional Data Assimilation)—LES is thoroughly described by Liu et al. [127]. They used simultaneously multi-scale nested model which allowed simulation of micro-scale circulations, in that case for the region of a farm. (2) Up-scale a CWE model to include MEM capabilities—co-called: single-model up-scaling. This method was considered in details by Mochida et al. [128] who also presented several examples of its use for wind engineering purposes, like the mitigation of snow disaster in urban environment and the local area wind energy prediction system. The first problem was described thoroughly by Tominaga et al. [129]. (3) Down-scale an MEM model to include the CWE model capabilities— co called: single-model downscaling. In methods (2) and (3) phenomena related to meso-scale and CWE are realized by nesting the computational domains. (4) Hybrid method which combines above three methods. Yamada and Koke [126] illustrated down-scaling and hybrid methods by a few examples.

More recently coupled meso- (WRF) and micro-scale (LES) simulations were performed by Mughal et al. [130] who studied configuration of the wind farm placed at Lake Turkana in Africa. Baik et al. [131] used downscaled data from MM5 to provide boundary conditions in nested RANS model to simulate flow and dispersion in a dense urban area of Seoul. Another example of downscaling approach was presented by Tewari et al. [132] who used WRF data as boundary conditions for CFD to simulate contaminant transport and dispersion over complex urban terrain of Salt Lake City and by Chahine et al. [133] who also used WRF and CFD to examine flow features over suburban terrain. The flow over complex terrain simulated by different RANS models with the meso-scale inflow conditions (WRF) was performed also by Temel et al. [134]. Coupled WRF and three different CFD approaches simulations were conducted by Gopalan et al. [135] to predict wind turbine power. CFD air quality simulations with regard to pollutants over the urban terrain with high-rise buildings in Seoul were carried out by Kwak et al. [136] who used downscaled data from WRF.

For the behavior of wildland fires the most import factors are the wind speed and its direction affected by the terrain topography. There are a few models which allow estimation of fire propagation (e.g.: FARSITE, FireStation, Wildfireanalyst, CARDIN, BEHAVE, Prometheus, etc.). The application of these models requires more exact definition of wind parameters than it is performed in meso-scale. A WindNinja is a wind simulation model which supports wildland fires operation. It takes into account the influence of terrain on the flow and dynamically down-scales data from meso-scale and provides a good resolution. The bases of the model, comparisons of various approaches to simulate wind in wildland fires and model applications are described in the papers by Forthofer et al. [137, 138], Wagenbrenner et al. [139]. Coupling between FARSITE model of the fire propagation and the wind simulator WindNinja and several proposals of improvements of this coupling was discussed in papers by Sanjuan et al. [140–142], Brun et al. [143].
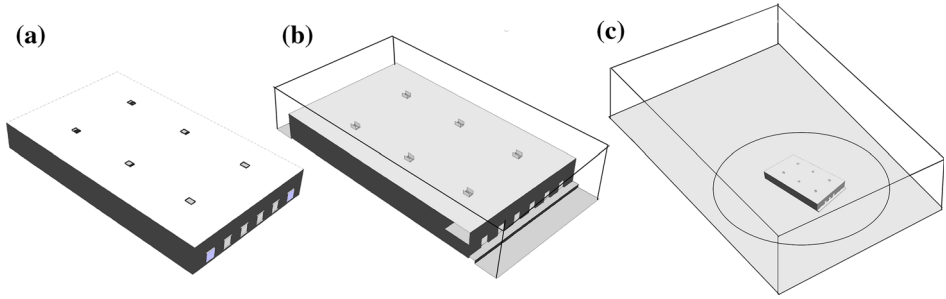
Figure 9.   Three approaches to the creation of numerical domain used in modelling NSHEVS in fire and wind coupling simulations [144].

# 7. Procedures for Wind and Fire Coupling in CFD Modelling

7.1. *Preparation of the Case*

In various cases, a different level of detail and in consequence a different accuracy of description of air flow can be used. In some cases, the user is interested only in the most basic effect of opposing wind—the pressure changes on the model boundaries. In this case, modelling the whole domain may be too costly. Conversely, as was already mentioned, the proper determination of pressure requires building the domain with the appropriate dimensions. In [144], based on a case study on modelling natural smoke ventilation in an industrial building, the authors determined three approaches that differ with the level of detail of the numerical domain, Figs. 9 and 10:

(a) The model is simplified to include only the interior of the building. Outlets are modelled as pressure boundary conditions, wind is introduced as a pressure gradient at the boundary.
(b) The model is simplified to include the interior of the building and the nearest exterior domain. Outlets are modelled as openings in the walls, along with their most essential features. Pressure boundaries are at the edges of the domain. The size of the domain is insufficient for CWE purposes, wind is introduced as a constant velocity or a vertical velocity profile at the boundary of the domain. This approach may be suitable for analysis in which the build-

Figure 10.   Illustrations of three approaches to wind and fire ▶ coupling on practical examples: (a) interior of a sports hall, (b) rail station located at an urban canyon, (c) shopping mall located in a dense urban location. Figures present numerical models (left side) and results (right side) of smoke mass density plots (0 g/m^3 to 0.20 g/m^3) at 20th minute of each analysis. Works based on [146, 177, 178].

(a) Domain includes only the interior of the building – outlets modelled as pressure boundary conditions
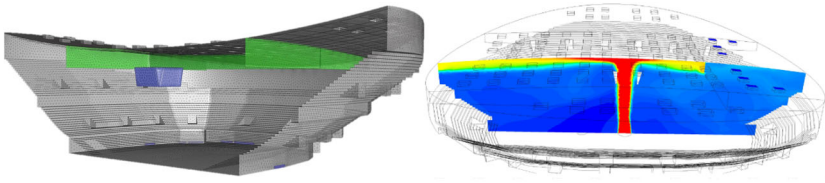
(b) Domain extends outside of the modelled space. Oblique wind angle analysis, however, is not possible, and wind is introduced as a constant velocity at the boundary. This railroad station was located in a large urban canyon.
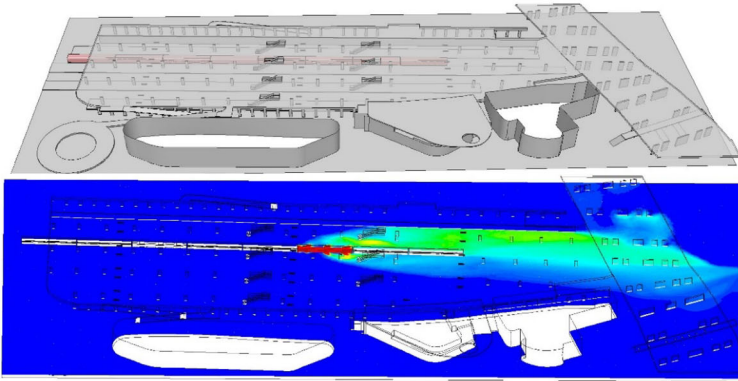
(c) Domain extends to the surrounding urban terrain, wind angle sensitivity study is possible, wind is introduced as a logarithmic profile at the domain boundary. The building was placed in a dense, urban development.
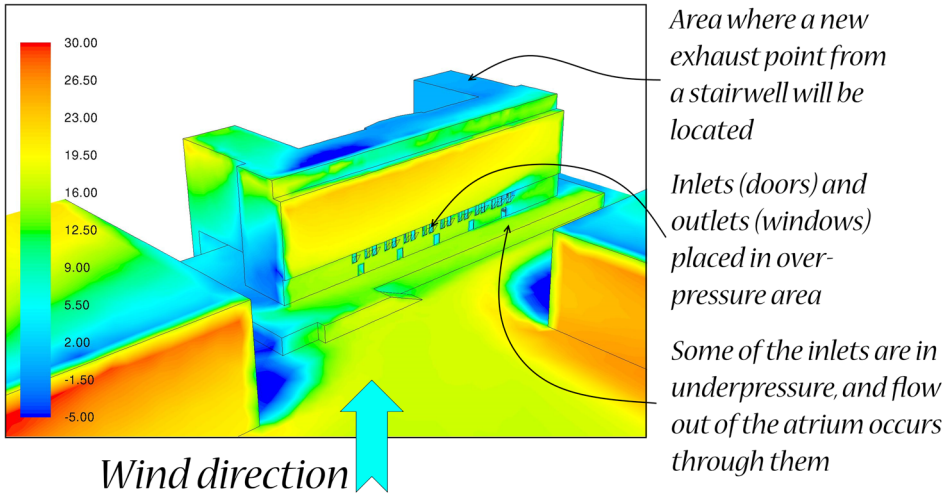

| 0.00 | 0.03 | 0.07 | 0.10 | 0.13 | 0.17 | 0.20 |
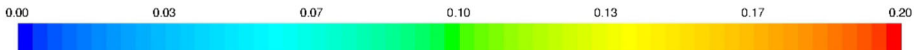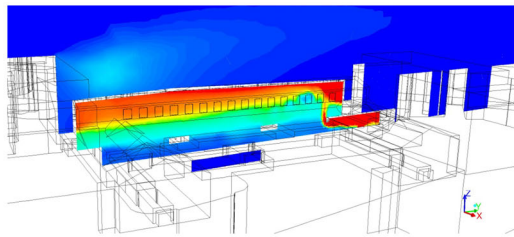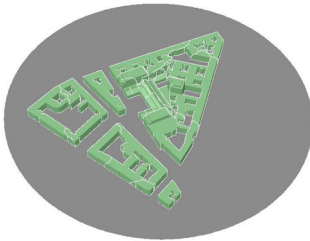
ing of interest lies in an ''urban canyon''. More details of the application of this approach can be found in the paper by Revuz et al. [70].

(c) The explicitly modelled part is placed within the large numerical domain. This type of modelling is suitable for CWE analysis, as the exterior domain is large enough to not influence the flow around the building. The building outlets have to be modelled in detail as physical openings with all of their distinctive features. The respective features of flow, like the wind profile, $u(z)$, turbulent kinetic energy, $k(z)$, its dissipation, $\varepsilon(z)$, should be modelled at the inlet to the domain.

The first approach (a) is sufficient only for the most basic, preliminary analysis, without taking into account wind influence. The simplification in the modelling of the inlets and outlets will strongly influence the performance of natural vents. The second method (b) is valid for the analysis of the performance of natural smoke control, but with limited ability to assess wind interaction. This method can be used for checking the tenability inside of the building, but the designer must add a margin of safety to the results, as in wind conditions they may be significantly worse. The introduction of wind velocity in such an approach will lead to its increase at the walls, due to flow compression. Also, the pressure effects at the walls will not be resolved correctly and neither will any effects of the surrounding buildings. In some rare cases, such as when the building and all of its inlets/outlets lie in a region of an ''urban canyon'', this approach may be sufficient. Otherwise, approach (c) is recommended. The building of interest is modelled as a complete assembly—with all of the internal features that may take part in the transport of smoke (compartments, corridors, atria and their internal openings). The outside of the building may be open (if a remote building is considered) or explicitly modelled in case of urban location. The size of the domain should be sufficient to resolve the upstream and downstream flow, and the model should allow investigation of the effects at oblique angles of wind attack. This approach is also valid for modelling wildfires or urban dispersion of smoke and other combustion products. Practical examples of simulations employing all three approaches are shown on Fig. 10.

7.2. Preliminary Wind Analysis

It is impossible to propose a rule of thumb for the wind direction, which will form the worst condition for the fire. The flows inside a building and in its proximity depend on the pressure at the building inlets, such as doors, windows and ventilators and the forces acting due to the fire (Fig. 11). The building surroundings and the terrain will affect the flow as well, and a different outcome may be expected with every different wind angle. For simple buildings and simple combinations of buildings, it is possible to obtain, through the hand calculation methodology presented in Eurocode 1–4 [145], approximated values of pressure on the facades. For more complex structures and urban environments, CFD analysis is necessary. For a good representation of the different possibilities of wind action, no less than 12 wind angles should be considered [146].

| 30.00 |
| 26.50 |
| 23.00 |
| 19.50 |
| 16.00 |
| 12.50 |
| 9.00 |
| 5.50 |
| 2.00 |
| -1.50 |
| -5.00 |

Area where a new exhaust point from a stairwell will be located

Inlets (doors) and outlets (windows) placed in over-pressure area

Some of the inlets are in underpressure, and flow out of the atrium occurs through them

Wind direction

Figure 11. Example results of step 1 of the analysis—the pressure values at model boundaries. Inlets and outlets to the interior of the building are visible (doors and windows).

For buildings, tunnels and urban analyses, the investigation of multiple wind attack angles in a transient, fire simulation is a very time- and CPU power-consuming task. In order to reduce the computational cost, the analysis may be divided into two steps. First step is a preliminary steady-state analysis of wind flow in the domain (and induced indoor flows), to determine the most unfavourable wind angles. Second step is a transient analysis with the representation of the fire, for the worst angles of wind.

In the first step, wind analysis without a fire is performed to evaluate wind influence over the external features of the building. This simulation may be carried out according to two approaches—coupled and decoupled [4]. In the coupled approach, the numerical domain contains both the exterior and the interior of the model, which are connected through inlets. In this approach, the solver will resolve the indoor flows. As this simulation is performed in ambient temperatures, the flows may differ from the results obtained in the fire simulation, due to the lack of buoyant forces generated by the fire. This approach requires a high-quality mesh and detailed domain, but due to the fact that fire does not have to be resolved, it is significantly cheaper than the transient, fire-oriented CFD. In the decoupled approach, the domain contains only the exterior, and the interior may be resolved in a separate model (or just discarded). In this case, the user assumes that openings are sealed, which may lead to different results than in the case when the building with its interior is modelled as coupled. As a general recommendation, the coupled approach is prevalent in wind engineering [2] and, thus, also recommended.

The results of Step 1 should be investigated, with regards to pressure on the building inlets and outlets, as well as the indoor flows induced by the wind. The analysis itself is steady-state and the averaged conditions and flow features are estimated. The results of such a study are investigated with respect to wind pressure coefficient values in areas where elements of the natural smoke exhaust system are located. The worst scenario is usually one with the highest pressure on the ventilators, the highest suction near inlet air openings or with the highest air velocity inside the building. It is possible that this analysis will indicate multiple scenarios to be evaluated in further CFD studies. Once the worst-case scenario (or scenarios) are determined, the transient simulation with the fire inside the building can be performed.

7.3. Fire/Wind Coupled Simulations

Wind/fire CFD study must be performed as a coupled simulation, which means that the interior and exterior of the building must be explicitly modelled within the domain and physically connected to each other through openings. The challenges lie with the significant differences of scales between the domain, which allow the resolution of the wind and the interior features of the buildings, required to resolve the fire-induced buoyant flows [147] and ceiling jets [148].

The complete description of fire-related CFD modelling is beyond the scope of this review paper. The resources of knowledge on modelling fire-related phenomena are the works of Karlsson and Quintiere [149], Quintiere [150], Babrauskas [151] and Drysdale [152]. For a summary of the approaches to modelling in FSE, the reader may refer to the review elaborated by Węgrzyński and Sulik [153]. A review on the CFD modelling of fire, with emphasis on the mathematical models used in FDS software, was published by McGrattan et al. [80], and in a more general form by McGrattan and Miles [154], and Sztarbała [155]. The use of CFD in FSE was also thoroughly reviewed by Merci and Beji [156]. The FDS solver documentation, including the validation guide, is an invaluable source of knowledge on the approaches used in fire modelling [73, 75]. For the tenability criteria used in fire-related CFD, the reader is redirected to [157–160]. Some recent work related to the application of CFD in cases that are related to the topic of this review is presented in [161–164]. The literature presented here can be considered as ''the tip of the iceberg'' of the vast literature in the field of fire safety engineering, related to the modelling of fires, and should not be considered as an exhaustive list.

The goals of CFD analysis differ, depending on the subject of the analysis (e.g. building, tunnel, urban habitat or WUI area). In simulations of buildings, the goals usually are to evaluate the possibility and the conditions in which an evacuation will take place. This is commonly investigated through tenability criteria, and the concept of Available and Required Save Evacuation Times (respectively ASET and RSET). The ASET is the period between the occurrence of the fire, and the moment when the conditions within the building are untenable and evacuation is not possible. The RSET is the period of time required to evacuate people from a building. The building may be considered safe, if ASET is larger than RSET, with a sufficient margin of safety. The concept of ASET/RSET was intro-

duced in the 1980s by Cooper [165, 166], and since then it has been prevalent in determining the fire safety of buildings, despite the known limitations of this approach [167–169]. In addition to the investigation of tenability criteria, a building's fire and wind analysis should also focus on indoor flows caused by wind and fire interaction.

CFD simulations of fires in naturally ventilated buildings may also be used to determine the performance of natural ventilators [170], as well as investigate possible solutions to prevent adverse wind effects [171]. One must note that it is impossible to estimate the discharge coefficient C_v of a vent mounted on a building due to the inherent limitations of the discharge coefficient test method, described in detail in Part 1. One may, however, use CFD modelling to compare mass flow through a ventilator with and without wind influence, in order to evaluate the potential drop in performance, and investigate countermeasures.

In the case of urban dispersion modelling (smoke, pollutants etc.), the main target of the analysis is the time and spatial distribution of smoke and toxic pollutants, and the determination of possible radiative heat flux from the fire. In these simulations, the tenability criteria are usually assessed for the chosen targets (e.g. buildings, roads, critical infrastructure). The criteria for assessment must be evaluated individually for each simulation—in some cases, the criteria appropriate for buildings will be sufficient, whereas in others, no exposure to smoke can be expected. CFD computations that include wind and fire in an urban environment may be used a priori to estimate release from a potential source, or a posteriori to model the consequences of a release that has occurred. In the first case, the goal is to find preventive measures, and in the second it may be the mitigation of damage. More information on modelling the dispersion of toxic gases, coupled with evacuation modelling, can be found in the works of Lovreglio et al. [172], and Mouilleau and Champassith [173].

In wildfire modelling, the primary goal is to investigate the influence of wind on fire spread (through radiation or direct flame contact) and the transport of burning embers. Another goal of wildfire-related CFD may be to investigate the transport of smoke from a fire towards human habitat, or potential evacuation paths. In the latter case, the same approach as for urban dispersion modelling may be used, i.e. the determination of targets and the estimation of the tenability (or ignition) criteria for these. The transport of embers may be accomplished through the introduction of Lagrangian particles into the model [174, 175]. Another meaningful use of CFD modelling of fire in wind conditions is operational forest fire modelling, described in more detail in Part 1. This approach utilises real-time measurements of meteorological meso-scale conditions and their assimilation to define boundary conditions, and uses CFD to predict the spread of fire [176].

8. Conclusions

Coupled wind and fire modelling for fire safety engineering applications is a challenging and arduous task. Multiple difficulties arise when good practice guidelines elaborated for wind engineering have to be introduced into a typical fire safety

CFD routine. They are: (1) the size of the domain, (2) the high quality of the computational mesh especially in areas of deatachment and reatachment of the flow, (3) the boundary layer, which is generated at the inlet to the domain and should remain unchanged along the whole fetch, (4) modelling the terrain roughness to maintain correct wind profile or (5) the introduction of wind angle sensitivity analysis, to name a few.

The routine presented in this paper can be considered as an excerpt from multiple best practice guidelines available for wind engineering, covering the most important aspects relevant to FSE. Following this routine does not guarantee, that the results of the study will be accurate; however, it can significantly limit the most common sources of error in wind related CFD simulations. The approach presented herein may be beneficial to both scientists and engineers, and this approach has already been successfully used in practice in some of the referred studies. Moreover, shortly before the commission of this research paper, the most popular fire-oriented CFD code FDS has received an update related to wind modelling, including new boundary condition (WIND), that has significantly simplified the introduction of wind characteristics into numerical models. The considerations presented in this paper may be helpfull, to fully benefit from these new capabilities.

Some important gaps in knowledge were identified within this literature review, most notably:

1. There is a lack of high quality experimental data that would include both fire and wind related measurements, and which could be useful for model validation. Existing studies either cover multiple wind angles or velocities, and have very limited data related to fire, or consist of singular fire experiments conducted in windy conditions, with wind velocity being registered. There is a lack of data in which both wind and fire would be parameters in high resolution parametric studies. It is difficult to conduct such analyses in full scale, however, the use of wind tunnel experiments to validate the numerical model in ambient temperature, and further performance of fire related parametric numerical study seems as a feasible alternative to costly full-scale research, and difficult model scale fire experiments in wind tunnels.

2. Some of the rules presented in this paper, such as the recommendations for the size of the domain, may be too restrictive. There is insufficient data related to the consequences of the change in the size of the domain, use of periodic boundary conditions at the boundaries or use of scaled down models. As fire related CFD is usually performed as transient analysis, it has higher computational cost than typical steady-state solution for determination of pressure coefficients in wind engineering. Thus, the imperative for domain and mesh otpimisation may be stronger for fire engineering applications, than for typical CWE analyses. Nevertheless, until more information is gathered in this field, it is advised to follow the recommendations of CWE best practice guidelines, or perform own sensitivity studies.

3. The tenability criteria for the interior of buildings are generally well defined within the FSE community, although such criteria may not always be used to

the external domain (e.g. path of escape for WUI area, urban area near smoke exhaust points). Some researchers use "no exposure" condition, in other cases researchers refer to various contaminant concentrations, from No Observable Adverse Effect Level (NOAEL) to lethal concentrations (e.g. FED = 1, LC_{50}), and others to common tenability criteria for buildings. It is not defined, what exposure to smoke from fire incident is acceptable. This gap is a difficult problem for risk based analysis of the smoke release in urban environments.

4. A difficult aspect of wind/fire coupled modeling is the introduction of the wind into numerical domain—either from statistical data, historical records or on-site measurements. The scalling methods which allow to apply wind data in ABL models in CFD analyses (micro-scale) seem promising, however there is a need for further development of such models to allow for quick and reliable data transfer from measurements into CFD models. Improved meso-scale models and wind/fire CFD analysis would allow for better planning, preparedness and emergency response.

5. An emerging related field of research are environmental studies on the spread of smoke in global scale, focused mainly on the consequences of the long range smoke dispersion in the atmosphere. This issue in wind engineering encounters similar problems with scaling meso-scale data as it was mentioned in previous point. The fire community should take active role in such research, as fire safety engineers may have important knowledge that could help to develop large scale fire models and improve the climate predictions. This could allow building a bridge between CWE and FSE areas, which could help further improvements in the models used for wind/fire coupled analyses.

As it was shown in the both parts of the review, there are cases in which the extraordinary effort to combine wind and fire engineering is highly beneficial. Firstly, the use of combined wind and fire engineering allows for the development of efficient natural smoke control systems that would be impossible otherwise. Secondly, with increasing attention paid towards the environment, the ability to model the large-scale effects of fires, beyond the buildings in which they take place, will be expected from engineers in the foreseeable future. Also, as computational capabilities increase with time, and access to higher resolution meteorological data is easier, the operational modelling of fire disasters (large fires, conflagrations, wildfires) will be more accessible. This is a tool that will be used not only to design better buildings or technical solutions but will be directly involved in safeguarding the surrounding nature and saving lives. Finally, it may be concluded that further development of many FSE-related problems will strongly depend on our ability to model wind and its effects properly.

References

1. Weinschenk CG, Overholt KJ, Madrzykowski D (2015) Simulation of an attic fire in a wood frame residential structure, Chicago, IL. Fire Technol 52:1629–1658. https://doi.org/10.1007/s10694-015-0533-7

2. Blocken B (2014) 50 years of computational wind engineering: past, present and future. J Wind Eng Ind Aerodyn 129:69–102. https://doi.org/10.1016/j.jweia.2014.03.008

3. Franke J, Hirsch C, Jensen AG, Krus HW, Schatzmann M, Westbury PS, Miles SD, Wisse JA, Wright NG (2004) Recommendations on the use of CFD in wind engineering. In: van Beeck JPAJ (ed) Proceedings of the international conference on urban wind engineering and building aerodynamics. COST action C14, impact of wind and storm on city life built environment, pp 1–11

4. Ramponi R, Blocken B (2012) CFD simulation of cross-ventilation for a generic isolated building: impact of computational parameters. Build Environ 53:34–48. https://doi.org/10.1016/j.buildenv.2012.01.004

5. Blocken B (2015) Computational fluid dynamics for urban physics: importance, scales, possibilities, limitations and ten tips and tricks towards accurate and reliable simulations. Build Environ 91:219–245. https://doi.org/10.1016/j.buildenv.2015.02.015

6. Tominaga Y, Mochida A, Yoshie R, Kataoka H, Nozu T, Yoshikawa M, Shirasawa T (2008) AIJ guidelines for practical applications of CFD to pedestrian wind environment around buildings. J Wind Eng Ind Aerodyn 96:1749–1761. https://doi.org/10.1016/j.jweia.2008.02.058

7. Franke J, Hellsten A, Schlünzen H, Carissimo B (2007) Best practice guideline for the CFD simulation of flows in the urban environment. COST Office Brussels

8. Franke J, Hellsten A, Schlünzen KH, Carissimo B (2011) The COST 732 best practice guideline for CFD simulation of flows in the urban environment: a summary. Int J Environ Pollut 44:419. https://doi.org/10.1504/IJEP.2011.038443

9. Mochida A, Tominaga Y, Murakami S, Yoshie R, Ishihara T, Ooka R (2002) Comparison of various k–ε models and DSM applied to flow around a high-rise building—report on AIJ cooperative project for CFD prediction of wind environment. Wind Struct 5:227–244. https://doi.org/10.12989/was.2002.5.2_3_4.227

10. Tominaga Y, Mochida A, Shirasawa T, Yoshie R, Kataoka H, Harimoto K, Nozu T (2004) Cross comparisons of CFD results of wind environment at pedestrian level around a high-rise building and within a building complex. J Asian Archit Build Eng 70:63–70. https://doi.org/10.3130/jaabe.3.63

11. Yoshie R, Mochida A, Tominaga Y, Kataoka H, Harimoto K, Nozu T, Shirasawa T (2007) Cooperative project for CFD prediction of pedestrian wind environment in the Architectural Institute of Japan. J Wind Eng Ind Aerodyn 95:1551–1578. https://doi.org/10.1016/j.jweia.2007.02.023

12. Tamura T (2008) Towards practical use of LES in wind engineering. J Wind Eng Ind Aerodyn 96:1451–1471. https://doi.org/10.1016/j.jweia.2008.02.034

13. Blocken B, Janssen WD, van Hooff T (2012) CFD simulation for pedestrian wind comfort and wind safety in urban areas: general decision framework and case study for the Eindhoven University campus. Environ Model Softw 30:15–34. https://doi.org/10.1016/j.envsoft.2011.11.009

14. Tominaga Y, Blocken B (2015) Wind tunnel experiments on cross-ventilation flow of a generic building with contaminant dispersion in unsheltered and sheltered conditions. Build Environ 92:452–461. https://doi.org/10.1016/j.buildenv.2015.05.026

15. Tominaga Y, Blocken B (2016) Wind tunnel analysis of flow and dispersion in cross-ventilated isolated buildings: impact of opening positions. J Wind Eng Ind Aerodyn 155:74–88. https://doi.org/10.1016/j.jweia.2016.05.007

16. van Hooff T, Blocken B, Tominaga Y (2017) On the accuracy of CFD simulations of cross-ventilation flows for a generic isolated building: comparison of RANS, LES and experiments. Build Environ 114:148–165. https://doi.org/10.1016/j.buildenv.2016.12.019

17. Uematsu Y, Watanabe K, Sasaki A, Motohiko Y, Hongo T (1999) Wind-induced dynamic response and resultant load estimation of a circular flat roof. J Wind Eng Ind Aerodyn 83:251–261. https://doi.org/10.1016/S0167-6105(99)00076-8

18. Uematsu Y, Moteki T, Hongo T (2008) Model of wind pressure field on circular flat roofs and its application to load estimation. J Wind Eng Ind Aerodyn 96:1003–1014. https://doi.org/10.1016/j.jweia.2007.06.025

19. Richards PJ, Hoxey RP (2006) Flow reattachment on the roof of a 6 m cube. J Wind Eng Ind Aerodyn 94:77–99. https://doi.org/10.1016/j.jweia.2005.12.002

20. Richards PJ, Hoxey RP (2008) Wind loads on the roof of a 6 m cube. J Wind Eng Ind Aerodyn 96:984–993. https://doi.org/10.1016/j.jweia.2007.06.032

21. Gerhardt H, Kramer C (1992) Effects of building geometry on roof wind loading. J Wind Eng Ind Aerodyn 41–44:1765–1773

22. Lipecki T (2013) Pressure coefficient on flat roofs of rectangular buildings. In: 6th European and African conference on wind engineering. Robinson College, Cambridge, pp 1–8

23. Stathopoulos T, Marathe R, Wu H (1999) Mean wind pressures on flat roof corners affected by parapets: field and wind tunnel studies. Eng Struct 21:629–638. https://doi.org/10.1016/S0141-0296(98)00011-X

24. Kareem A, Lu PC (1992) Pressure fluctuations on flat roofs with parapets. J Wind Eng Ind Aerodyn 41–44:1775–1786

25. Pindado S, Meseguer J (2003) Wind tunnel study on the influence of different parapets on the roof pressure distribution of low-rise buildings. J Wind Eng Ind Aerodyn 91:1133–1139. https://doi.org/10.1016/S0167-6105(03)00055-2

26. Blessing C, Chowdhury AG, Lin J, Huang P (2009) Full-scale validation of vortex suppression techniques for mitigation of roof uplift. Eng Struct 31:2936–2946. https://doi.org/10.1016/j.engstruct.2009.07.021

27. Mooneghi MA, Irwin P, Chowdhury AG (2014) Large-scale testing on wind uplift of roof pavers. J Wind Eng Ind Aerodyn 128:22–36. https://doi.org/10.1016/j.jweia.2014.03.001

28. Cao J, Tamura Y, Yoshida A (2012) Wind pressures on multi-level flat roofs of medium-rise buildings. J Wind Eng Ind Aerodyn 103:1–15. https://doi.org/10.1016/j.jweia.2012.01.005

29. Cao J, Tamura Y, Yoshida A (2013) Wind tunnel investigation of wind loads on rooftop model modules for green roofing systems. J Wind Eng Ind Aerodyn 118:20–34. https://doi.org/10.1016/j.jweia.2013.04.006

30. Pindado S, Meseguer J, Franchini S (2011) Influence of an upstream building on the wind-induced mean suction on the flat roof of a low-rise building. J Wind Eng Ind Aerodyn 99:889–893. https://doi.org/10.1016/j.jweia.2011.06.003

31. Wu F, Sarkar PP, Mehta KC, Zhao Z (2001) Influence of incident wind turbulence on pressure fluctuations near flat-roof corners. J Wind Eng Ind Aerodyn 89:403–420. https://doi.org/10.1016/S0167-6105(00)00072-6

32. Tieleman HW, Reinhold TA, Hajj MR (2001) Detailed simulation of pressures in separated/reattached flows. J Wind Eng Ind Aerodyn 89:1657–1670

33. Tieleman HW, Ge Z, Hajj MR, Reinhold TA (2003) Pressures on a surface-mounted rectangular prism under varying incident turbulence. J Wind Eng Ind Aerodyn 91:1095–1115. https://doi.org/10.1016/S0167-6105(03)00045-X

34. Kawai H (2002) Local peak pressure and conical vortex on building. J Wind Eng Ind Aerodyn 90:251–263. https://doi.org/10.1016/S0167-6105(01)00218-5

35. Banks D, Meroney RN, Sarkar PP, Zhao Z, Wu F (2000) Flow visualization of conical vortices on flat roofs with simultaneous surface pressure measurement. J Wind Eng Ind Aerodyn 84:65–85. https://doi.org/10.1016/S0167-6105(99)00044-6

36. Stathopoulos T, Zhou YS (1995) Numerical evaluation of wind pressures on flat roofs with the k–ε model. Build Environ 30:267–276. https://doi.org/10.1016/0360-1323(94)00038-T

37. Ono Y, Tamura T, Kataoka H (2008) LES analysis of unsteady characteristics of conical vortex on a flat roof. J Wind Eng Ind Aerodyn 96:2007–2018. https://doi.org/10.1016/j.jweia.2008.02.021

38. Richards PJ, Hoxey RP, Short LJ (2001) Wind pressures on a 6 m cube. J Wind Eng Ind Aerodyn 89:1553–1564. https://doi.org/10.1016/S0167-6105(01)00139-8

39. Richards PJ, Hoxey RP (2002) Unsteady flow on the sides of a 6 m cube. J Wind Eng Ind Aerodyn 90:1855–1866. https://doi.org/10.1016/S0167-6105(02)00293-3

40. Richards PJ, Hoxey RP, Connell BD, Lander DP (2007) Wind-tunnel modelling of the Silsoe Cube. J Wind Eng Ind Aerodyn 95:1384–1399. https://doi.org/10.1016/j.jweia.2007.02.005

41. Richards PJ, Hoxey RP (2012) Pressures on a cubic building-part 1: full-scale results. J Wind Eng Ind Aerodyn 102:72–86. https://doi.org/10.1016/j.jweia.2011.11.004

42. Richards PJ, Hoxey RP (2012) Pressures on a cubic building-part 2: quasi-steady and other processes. J Wind Eng Ind Aerodyn 102:87–96. https://doi.org/10.1016/j.jweia.2011.11.003

43. Easom G (2000) Improved turbulence models for computational wind engineering. Ph.D. Thesis, The University of Nottingham

44. Wright NGG, Easom GJJ (2003) Non-linear k–ε turbulence model results for flow over a building at full-scale. Appl Math Model 27:1013–1033. https://doi.org/10.1016/S0307-904X(03)00123-9

45. Richards P, Norris S (2015) LES modelling of unsteady flow around the Silsoe cube. J Wind Eng Ind Aerodyn 144:70–78. https://doi.org/10.1016/j.jweia.2015.03.018

46. King MF, Gough HL, Halios C, Barlow JF, Robertson A, Hoxey R, Noakes CJ (2017) Investigating the influence of neighbouring structures on natural ventilation potential of a full-scale cubical building using time-dependent CFD. J Wind Eng Ind Aerodyn 169:265–279. https://doi.org/10.1016/j.jweia.2017.07.020

47. King M-F, Khan A, Delbosc N, Gough HL, Halios C, Barlow JF, Noakes CJ (2017) Modelling urban airflow and natural ventilation using a GPU-based lattice-Boltzmann method. Build Environ 125:273–284. https://doi.org/10.1016/j.buildenv.2017.08.048

48. Melbourne WH (1980) Comparison of measurements of the CAARC standard tall building model in simulated model wind flows. J Wind Eng Ind Aerodyn 6:78–88

49. Goliger AM, Milford RV (1988) Sensitivity of the CAARC standard building model to geometric scale and turbulence. J Wind Eng Ind Aerodyn 31:105–123

50. Tang UF, Kwok KCS (2004) Interference excitation mechanisms on a 3DOF aeroelastic CAARC building model. J Wind Eng Ind Aerodyn 92:1299–1314. https://doi.org/10.1016/j.jweia.2004.08.004

51. Huang S, Li QS, Xu S (2007) Numerical evaluation of wind effects on a tall steel building by CFD. J Constr Steel Res 63:612–627. https://doi.org/10.1016/j.jcsr.2006.06.033

52. Huang MF, Lau IWH, Chan CM, Kwok KCS, Li G (2011) A hybrid RANS and kinematic simulation of wind load effects on full-scale tall buildings. J Wind Eng Ind Aerodyn 99:1126–1138. https://doi.org/10.1016/j.jweia.2011.09.003

53. Daniels SJ, Castro IP, Xie ZT (2013) Peak loading and surface pressure fluctuations of a tall model building. J Wind Eng Ind Aerodyn 120:19–28. https://doi.org/10.1016/j.jweia.2013.06.014

54. Elshaer A, Aboshosha H, Bitsuamlak G, El Damatty A, Dagnew A (2016) LES evaluation of wind-induced responses for an isolated and a surrounded tall building. Eng Struct 115:179–195. https://doi.org/10.1016/j.engstruct.2016.02.026

55. Braun AL, Awruch AM (2009) Aerodynamic and aeroelastic analyses on the CAARC standard tall building model using numerical simulation. Comput Struct 87:564–581. https://doi.org/10.1016/j.compstruc.2009.02.002

56. Levitan MC, Mehta KC (1992) Texas Tech field experiments for wind loads. Part I. Building and pressure measuring system. J Wind Eng Ind Aerodyn 43:1565–1576

57. Levitan MC, Mehta KC (1992) Texas tech field experiments for wind loads. Part II. Meteorological instrumentation and terrain parameters. J Wind Eng Ind Aerodyn 43:1577–1588

58. Cochran LS, Cermak JE (1992) Full- and model-scale cladding pressures on the Texas Tech University experimental building. J Wind Eng Ind Aerodyn 41–44:1589–1600

59. Okada H, Ha Y-C (1992) Comparison of wind tunnel and full-scale pressure measurement tests on the Texas Tech Building. J Wind Eng Ind Aerodyn 41–44:1601–1612

60. Cheung JCK, Holmes JD, Melbourne WH (1997) Pressures on a 110 scale model of the Texas Tech Building. J Wind Eng Ind Aerodyn 71:529–538

61. Tieleman HW, Surry D, Mehta KC (1996) Full/model-scale comparison of surface pressures on the Texas Tech experimental building. J Wind Eng Ind Aerodyn 61:1–23. https://doi.org/10.1016/0167-6105(96)00042-6

62. Lin JX, Surry D, Tieleman HW (1995) The distribution of pressure near roof corners of flat roof low buildings. J Wind Eng Ind Aerodyn 56:235–265. https://doi.org/10.1016/0167-6105(94)00089-V

63. Lin JX, Surry D (1998) The variation of peak loads with tributary area near corners on flat low building roofs. J Wind Eng Ind Aerodyn 77–78:185–196. https://doi.org/10.1016/S0167-6105(98)00142-1

64. Endo M, Bienkiewicz B, Ham HJ (2006) Wind-tunnel investigation of point pressure on TTU test building. J Wind Eng Ind Aerodyn 94:553–578. https://doi.org/10.1016/j.jweia.2006.01.019

65. Selvam RP (1996) Computation of flow around Texas Tech building using k–epsilon and Kato–Launder k–epsilon turbulence model. Eng Struct 18:856–860

66. Selvam RP (1997) Computation of pressures on Texas Tech University building using large eddy simulation. J Wind Eng Ind Aerodyn 67–68:647–657. https://doi.org/10.1016/S0167-6105(97)00107-4

67. Stathopoulos T (1997) Computational wind engineering: past achievements and future challenges. J Wind Eng Ind Aerodyn 67–68:509–532. https://doi.org/10.1016/S0167-6105(97)00097-4

68. Senthooran S, Lee DD, Parameswaran S (2004) A computational model to calculate the flow-induced pressure fluctuations on buildings. J Wind Eng Ind Aerodyn 92:1131–1145. https://doi.org/10.1016/j.jweia.2004.07.002

69. Blocken B, Stathopoulos T, van Beeck JPAJ (2016) Pedestrian-level wind conditions around buildings: review of wind-tunnel and CFD techniques and their accuracy for wind comfort assessment. Build Environ 100:50–81. https://doi.org/10.1016/j.buildenv.2016.02.004

70. Revuz J, Hargreaves DM, Owen JS (2012) On the domain size for the steady-state CFD modelling of a tall building. Wind Struct An Int J 15:313–329. https://doi.org/10.12989/was.2012.15.4.313

71. Vanella M, Posa A, Balaras E (2014) Adaptive mesh refinement for immersed boundary methods. J Fluids Eng 136:40901. https://doi.org/10.1115/1.4026415
72. Vanella M, McDermott R, Forney G (2015) A cut-cell immersed boundary technique for fire dynamics simulation. In: APS division of fluid dynamics meeting abstracts, p L7.003
73. McGrattan K, Hostikka S, McDermott R, Floyd J, Weinschenk C, Overholt K (2017) Fire Dynamics Simulator User's Guide, 6th edn
74. McGrattan K, Hostikka S, McDermott R, Floyd J, Weinschenk C, Overholt K (2015) Fire Dynamics Simulator technical reference guide. Volume 2: verification, 6th edn. NIST Special Publication 1018
75. McGrattan K, Hostikka S, McDermott R, Floyd J, Weinschenk C, Overholt K (2015) Fire Dynamics Simulator technical reference guide. Volume 3: validation, 6th edn. NIST Special Publication 1018-3
76. Pope SB (2004) Ten questions concerning the large-eddy simulation of turbulent flows. New J Phys 6:35. https://doi.org/10.1088/1367-2630/6/1/035
77. Roache PJ (1994) Perspective: a method for uniform reporting of grid refinement studies. J Fluids Eng 116:405. https://doi.org/10.1115/1.2910291
78. Roache PJ (1997) Quantification of uncertainty in computational fluid dynamics. Annu Rev Fluid Mech 29:123–160. https://doi.org/10.1146/annurev.fluid.29.1.123
79. van Hooff T, Blocken B (2010) Coupled urban wind flow and indoor natural ventilation modelling on a high-resolution grid: a case study for the Amsterdam ArenA stadium. Environ Model Softw 25:51–65. https://doi.org/10.1016/j.envsoft.2009.07.008
80. McGrattan K, McDermott R, Floyd J, Hostikka S, Forney G, Baum H (2012) Computational fluid dynamics modelling of fire. Int J Comput Fluid Dyn 26:349–361. https://doi.org/10.1080/10618562.2012.659663
81. Franke J (2007) Introduction to the prediction of wind loads on buildings by computational wind engineering (CWE). In: Stathopoulos T, Baniotopoulos CC (eds) Wind effects on buildings and design of wind-sensitive structures. Springer, Vienna, pp 67–103
82. Murakami S (1998) Overview of turbulence models applied in CWE-1997. J Wind Eng Ind Aerodyn 74–76:1–24. https://doi.org/10.1016/S0167-6105(98)00004-X
83. Argyropoulos CD, Markatos NC (2015) Recent advances on the numerical modelling of turbulent flows. Appl Math Model 39:693–732. https://doi.org/10.1016/j.apm.2014.07.001
84. Office of Nuclear Regulatory Research (2012) Computational fluid dynamics best practice guidelines for dry cask applications draft report for comment
85. Launder BE, Spalding JL (1972) Lectures in mathematical models of turbulence. Academic Press, New York
86. Yakhot V, Orszag SAA, Thangam S, Gatski TBB, Speziale CGG (1992) Development of turbulence models for shear flows by a double expansion technique. Phys Fluids A Fluid Dyn 4:1510. https://doi.org/10.1063/1.858424
87. Shih TH, Liou WW, Shabbir A, Yang Z, Zhu J (1995) A new k–e eddy viscosity model for high Reynolds number turbulent flows. Comput Fluids 24:227–238
88. Wilcox DC (1988) Re-assessment of the scale-determining equation for advanced turbulence models. AIAA J 26:1299–1310
89. Menter FR (1994) Two-equation eddy-viscosity turbulence models for engineering applications. AIAA J 32:1598–1605. https://doi.org/10.2514/3.12149
90. Smagorinsky J (1963) General circulation experiments with the primitive equations. I. The basic experiment. Mon Weather Rev 91:99–164

91. Germano M, Piomelli U, Moin P, Cabot WH (1991) A dynamic subgrid-scale eddy viscosity model. Phys Fluids A 3:1760–1765

92. Sarwar M, Moinuddin K, Thorpe GR (2013) Large eddy simulation over backwards facing step using fire dynamics simulator (FDS). In: Fourteenth Asian congress of fluid dynamics, pp 469–474

93. Toms BA (2015) Large-eddy simulation of flow over a backward facing step: assessment of inflow boundary conditions, eddy viscosity models, and wall functions. J Appl Mech Eng . https://doi.org/10.4172/2168-9873.1000169

94. Tamura T, Nozawa K, Kondo K (2008) AIJ guide for numerical prediction of wind loads on buildings. J Wind Eng Ind Aerodyn 96:1974–1984. https://doi.org/10.1016/j.jweia.2008.02.020

95. Spalart PR (2009) Detached-eddy simulation. Annu Rev Fluid Mech 41:181–202. https://doi.org/10.1146/annurev.fluid.010908.165130

96. Blocken B, Stathopoulos T, Carmeliet J (2007) CFD simulation of the atmospheric boundary layer: wall function problems. Atmos Environ 41:238–252. https://doi.org/10.1016/j.atmosenv.2006.08.019

97. Wieringa J (1992) Updating the Davenport roughness classification. J Wind Eng Ind Aerodyn 41:357–368. https://doi.org/10.1016/0167-6105(92)90434-C

98. Richards PJ, Hoxey RP (1993) Appropriate boundary conditions for computational wind engineering models using the k–ε turbulence model. In: Computational wind engineering 1. Elsevier, Amsterdam, pp 145–153

99. Porté-Agel F, Wu Y-T, Lu H, Conzemius RJ (2011) Large-eddy simulation of atmospheric boundary layer flow through wind turbines and wind farms. J Wind Eng Ind Aerodyn 99:154–168. https://doi.org/10.1016/j.jweia.2011.01.011

100. Shur ML, Spalart PR, Strelets MK, Travin AK (2014) Synthetic turbulence generators for RANS-LES interfaces in zonal simulations of aerodynamic and aeroacoustic problems. Flow Turbul Combust 93:63–92. https://doi.org/10.1007/s10494-014-9534-8

101. Tabor GR, Baba-Ahmadi MH (2010) Inlet conditions for large eddy simulation: a review. Comput Fluids 39:553–567. https://doi.org/10.1016/j.compfluid.2009.10.007

102. Dyer AJ (1974) A review of flux-profile relationships. Bound Layer Meteorol 7:363–372. https://doi.org/10.1007/BF00240838

103. Richards PJ, Norris SE (2011) Appropriate boundary conditions for computational wind engineering models revisited. J Wind Eng Ind Aerodyn 99:257–266. https://doi.org/10.1016/j.jweia.2010.12.008

104. Hargreaves DM, Wright NG (2007) On the use of the k–ε model in commercial CFD software to model the neutral atmospheric boundary layer. J Wind Eng Ind Aerodyn 95:355–369. https://doi.org/10.1016/j.jweia.2006.08.002

105. Yang Y, Gu M, Chen S, Jin X (2009) New inflow boundary conditions for modelling the neutral equilibrium atmospheric boundary layer in computational wind engineering. J Wind Eng Ind Aerodyn 97:88–95. https://doi.org/10.1016/j.jweia.2008.12.001

106. Parente A, Gorlé C, van Beeck J, Benocci C (2011) Improved k–ε model and wall function formulation for the RANS simulation of ABL flows. J Wind Eng Ind Aerodyn 99:267–278. https://doi.org/10.1016/j.jweia.2010.12.017

107. Richards PJ, Norris SE (2015) Appropriate boundary conditions for a pressure driven boundary layer. J Wind Eng Ind Aerodyn 142:43–52. https://doi.org/10.1016/j.jweia.2015.03.003

108. Deaves DM, Harris RI (1978) A mathematical model of the structure of strong winds. CIRIA, London

109. Bęc J, Lipecki T, Błazik-Borowa E (2011) Research on wind structure in the wind tunnel of wind engineering laboratory of Cracow University of Technology. J Phys Conf Ser 318:72003. https://doi.org/10.1088/1742-6596/318/7/072003

110. Tominaga Y, Mochida A, Murakami S, Sawaki S (2008) Comparison of various revised k–ε models and LES applied to flow around a high-rise building model with 1:1:2 shape placed within the surface boundary layer. J Wind Eng Ind Aerodyn 96:389–411. https://doi.org/10.1016/j.jweia.2008.01.004

111. CEN (2010) EN 1991-1-4:2005 + A1: Eurocode 1: actions on structures—part 1–4: general actions–wind actions

112. ASCE (2006) ASCE/SEI 7-05 minimum design loads for buildings and other structures

113. AS-NZS (2011) AS-NZS 1170-2 structural design actions—part 2: wind actions

114. AIJ (2004) AIJ-RBL-1996 recommendations for loads on buildings

115. ISO (2009) ISO 4354:2009 wind actions on structures

116. Dyrbye C, Hansen S (1997) Wind loads on structures. Wiley, New York

117. Holmes JD (2004) Wind loading of structures. Taylor & Francis, London

118. Simiu E, Scanlan RH (1996) Wind effects on structures. Wiley, New York

119. Tamura Y, Kareem A (2014) Advanced structural wind engineering. Springer, Berlin

120. Hangan H, Refan M, Jubayer C, Romanic D, Parvu D, LoTufo J, Costache A (2017) Novel techniques in wind engineering. J Wind Eng Ind Aerodyn 171:12–33. https://doi.org/10.1016/j.jweia.2017.09.010

121. Schlünzen KH, Grawe D, Bohnenstengel SI, Schlüter I, Koppmann R (2011) Joint modelling of obstacle induced and mesoscale changes—current limits and challenges. J Wind Eng Ind Aerodyn 99:217–225. https://doi.org/10.1016/j.jweia.2011.01.009

122. Masson V (2006) Urban surface modeling and the meso-scale impact of cities. Theor Appl Climatol 84:35–45. https://doi.org/10.1007/s00704-005-0142-3

123. Garuma GF (2017) Review of urban surface parameterizations for numerical climate models. Urban Clim . https://doi.org/10.1016/j.uclim.2017.10.006

124. Ryu YH, Bou-Zeid E, Wang ZH, Smith JA (2016) Realistic representation of trees in an urban canopy model. Bound Layer Meteorol 159:193–220. https://doi.org/10.1007/s10546-015-0120-y

125. Krayenhoff ES, Christen A, Martilli A, Oke TR (2014) A multi-layer radiation model for urban neighbourhoods with trees. Bound Layer Meteorol 151:139–178. https://doi.org/10.1007/s10546-013-9883-1

126. Yamada T, Koike K (2011) Downscaling mesoscale meteorological models for computational wind engineering applications. J Wind Eng Ind Aerodyn 99:199–216. https://doi.org/10.1016/j.jweia.2011.01.024

127. Liu Y, Warner T, Liu Y, Vincent C, Wu W, Mahoney B, Swerdlin S, Parks K, Boehnert J (2011) Simultaneous nested modeling from the synoptic scale to the LES scale for wind energy applications. J Wind Eng Ind Aerodyn 99:308–319. https://doi.org/10.1016/j.jweia.2011.01.013

128. Mochida A, Iizuka S, Tominaga Y, Lun IYF (2011) Up-scaling CWE models to include mesoscale meteorological influences. J Wind Eng Ind Aerodyn 99:187–198. https://doi.org/10.1016/j.jweia.2011.01.012

129. Tominaga Y, Mochida A, Okaze T, Sato T, Nemoto M, Motoyoshi H, Nakai S, Tsutsumi T, Otsuki M, Uamatsu T, Yoshino H (2011) Development of a system for predicting snow distribution in built-up environments: combining a mesoscale meteorological model and a CFD model. J Wind Eng Ind Aerodyn 99:460–468. https://doi.org/10.1016/j.jweia.2010.12.004

130. Mughal MO, Lynch M, Yu F, Sutton J (2018) Forecasting and verification of winds in an East African complex terrain using coupled mesoscale- and micro-scale models. J Wind Eng Ind Aerodyn 176:13–20. https://doi.org/10.1016/j.jweia.2018.03.006

131. Baik J-J, Park S-B, Kim J-J (2009) Urban flow and dispersion simulation using a CFD model coupled to a mesoscale model. J Appl Meteorol Climatol 48:1667–1681. https://doi.org/10.1175/2009JAMC2066.1

132. Tewari M, Kusaka H, Chen F, Coirier WJ, Kim S, Wyszogrodzki AA, Warner TT (2010) Impact of coupling a microscale computational fluid dynamics model with a mesoscale model on urban scale contaminant transport and dispersion. Atmos Res 96:656–664. https://doi.org/10.1016/j.atmosres.2010.01.006

133. Chahine A, Dupont E, Musson-Genon L, Legorgeu C, Carissimo B (2018) Long term modelling of the dynamical atmospheric flows over SIRTA site. J Wind Eng Ind Aerodyn 172:351–366. https://doi.org/10.1016/j.jweia.2017.09.004

134. Temel O, Bricteux L, van Beeck J (2018) Coupled WRF-OpenFOAM study of wind flow over complex terrain. J Wind Eng Ind Aerodyn 174:152–169. https://doi.org/10.1016/j.jweia.2018.01.002

135. Gopalan H, Gundling C, Brown K, Roget B, Sitaraman J, Mirocha JD, Miller WO (2014) A coupled mesoscale–microscale framework for wind resource estimation and farm aerodynamics. J Wind Eng Ind Aerodyn 132:13–26. https://doi.org/10.1016/j.jweia.2014.06.001

136. Kwak KH, Baik JJ, Ryu YH, Lee SH (2015) Urban air quality simulation in a high-rise building area using a CFD model coupled with mesoscale meteorological and chemistry-transport models. Atmos Environ 100:167–177. https://doi.org/10.1016/j.atmosenv.2014.10.059

137. Forthofer JM, Butler BW, Mchugh CW, Finney MA, Bradshaw LS, Stratton RD, Shannon KS, Wagenbrenner NS (2014) A comparison of three approaches for simulating fine-scale surface winds in support of wildland fire management. Part II. An exploratory study of the effect of simulated winds on fire growth simulations. Int J Wildl Fire 23:982–994. https://doi.org/10.1071/WF12090

138. Forthofer JM, Butler BW, Wagenbrenner NS (2014) A comparison of three approaches for simulating fine-scale surface winds in support of wildland fire management. Part I. Model formulation and comparison against measurements. Int J Wildland Fire 23:969–981. https://doi.org/10.1071/WF12089

139. Wagenbrenner NS, Forthofer JM, Lamb BK, Shannon KS, Butler BW (2016) Downscaling surface wind predictions from numerical weather prediction models in complex terrain with WindNinja. Atmos Chem Phys 16:5229–5241. https://doi.org/10.5194/acp-16-5229-2016

140. Sanjuan G, Brun C, Margalef T, Cortés A (2016) Determining map partitioning to minimize wind field uncertainty in forest fire propagation prediction. J Comput Sci 14:28–37. https://doi.org/10.1016/j.jocs.2016.01.006

141. Sanjuan G, Margalef T, Cortés A (2016) Applying domain decomposition to wind field calculation. Parallel Comput 57:185–196. https://doi.org/10.1016/j.parco.2016.05.013

142. Sanjuan G, Margalef T, Cortés A (2018) Wind field parallelization based on Schwarz alternating domain decomposition method. Future Gener Comput Syst 82:565–574. https://doi.org/10.1016/j.future.2016.12.041

143. Brun C, Margalef T, Cortés A (2013) Coupling diagnostic and prognostic models to a dynamic data driven forest fire spread prediction system. Procedia Comput Sci 18:1851–1860. https://doi.org/10.1016/j.procs.2013.05.354

144. Węgrzyński W, Krajewski G, Sulik P (2016) Case study 2—production and storage building (Poland). In: 11th conference on performance-based codes and fire safety design methods. SFPE, Warszawa
145. CEN (2005) EN 1991-1-4:2005 Eurocode 1: actions on structures—part 1–4: general actions–wind actions
146. Krajewski G, Węgrzyński W (2018) Use of computational fluid dynamics in optimization of natural smoke ventilation from a historical shopping mall—case study. AIP Conf Proc 1922:110009. https://doi.org/10.1063/1.5019112
147. Morgan HP (1986) The horizontal flow of buoyant gases toward an opening. Fire Saf J 11:193–200. https://doi.org/10.1016/0379-7112(86)90062-7
148. Alpert RL (1975) Turbulent ceiling-jet induced by large-scale fires. Combust Sci Technol 11:197–213. https://doi.org/10.1080/00102207508946699
149. Karlsson B, Quintiere JG (2000) Enclosure fire dynamics. CRC Press, Boca Raton
150. Quintiere JG (2006) Fundamentals of fire phenomena. Wiley, New York
151. Babrauskas V (2003) Ignition handbook. Fire Science Publishers, Issaquah
152. Drysdale DD (2011) An introduction to fire dynamics, 3rd edn. Wiley, New York
153. Węgrzyński W, Sulik P (2016) The philosophy of fire safety engineering in the shaping of civil engineering development. Bull Polish Acad Sci Tech Sci 64:719–730. https://doi.org/10.1515/bpasts-2016-0081
154. McGrattan K, Miles S (2016) Modeling fires using computational fluid dynamics (CFD). In: SFPE handbook of fire protection engineering. Springer, New York, pp 1034–1065
155. Sztarbała G (2013) An estimation of conditions inside construction works during a fire with the use of computational fluid dynamics. Bull Polish Acad Sci Tech Sci 61:155–160. https://doi.org/10.2478/bpasts-2013-0014
156. Merci B, Beji T (2016) Fluid mechanics aspects of fire and smoke dynamics in enclosures. CRC Press, Boca Raton
157. Kuligowski ED (2016) Human behavior in fire. In: Hurley MJ, Gottuk DT, Hall JR Jr, Harada K, Kuligowski ED, Puchovsky M, Torero JL, Watts JM Jr, Wieczorek CJ (eds) SFPE handbook of fire protection engineering. Springer, New York, pp 2070–2114
158. Yamada T, Akizuki Y (2016) Visibility and human behavior in fire smoke. In: SFPE handbook of fire protection engineering. Springer, New York, pp 2181–2206
159. Purser DA, McAllister JL (2016) Assessment of hazards to occupants from smoke, toxic gases, and heat. In: SFPE handbook of fire protection engineering. Springer, New York, pp 2308–2428
160. Węgrzyński W, Vigne G (2017) Experimental and numerical evaluation of the influence of the soot yield on the visibility in smoke in CFD analysis. Fire Saf J 91:389–398. https://doi.org/10.1016/j.firesaf.2017.03.053
161. Perez Segovia JF, Beji T, Merci B (2017) CFD simulations of pool fires in a confined and ventilated enclosure using the Peatross–Beyler correlation to calculate the mass loss rate. Fire Technol 53:1669–1703. https://doi.org/10.1007/s10694-017-0654-2
162. Bari S, Naser J (2005) Simulation of smoke from a burning vehicle and pollution levels caused by traffic jam in a road tunnel. Tunn Undergr Space Technol 20:281–290. https://doi.org/10.1016/j.tust.2004.09.002
163. Yu LX, Beji T, Zadeh SE, Liu F, Merci B (2016) Simulations of smoke flow fields in a wind tunnel under the effect of an air curtain for smoke confinement. Fire Technol 52:1–20. https://doi.org/10.1007/s10694-016-0598-y

164. Król M, Król A (2017) Multi-criteria numerical analysis of factors influencing the efficiency of natural smoke venting of atria. J Wind Eng Ind Aerodyn 170:149–161. https://doi.org/10.1016/j.jweia.2017.08.012

165. Cooper LY (1983) A concept for estimating available safe egress time in fires. Fire Saf J 5:135–144. https://doi.org/10.1016/0379-7112(83)90006-1

166. Cooper LY (1982) A mathematical model for estimating available safe egress time in fires. Fire Mater 6:135–144. https://doi.org/10.1002/fam.810060307

167. Babrauskas V, Fleming JM, Don Russell B (2010) RSET/ASET, a flawed concept for fire safety assessment. Fire Mater 34:341–355. https://doi.org/10.1002/fam.1025

168. Purser D (2003) ASET and RSET: addressing some issues in relation to occupant behaviour and tenability. Fire Saf Sci . https://doi.org/10.3801/IAFSS.FSS.7-91

169. Kuligowski ED, Gwynne SMV, Hulse LM, Kinsey MJ (2016) Guidance for the model developer on representing human behavior in egress models. Fire Technol 52:775–800. https://doi.org/10.1007/s10694-015-0501-2

170. Węgrzyński W, Krajewski G (2017) Influence of wind on natural smoke and heat exhaust system performance in fire conditions. J Wind Eng Ind Aerodyn 164:44–53. https://doi.org/10.1016/j.jweia.2017.01.014

171. Węgrzyński W, Krajewski G, Kimbar G (2018) A concept of external aerodynamic elements in improving the performance of natural smoke ventilation in wind conditions. AIP Conf Proc 1922:110006. https://doi.org/10.1063/1.5019109

172. Lovreglio R, Ronchi E, Maragkos G, Beji T, Merci B (2016) An integrated dynamic approach for the impact of a toxic gas dispersion hazard: coupling human behaviour and dispersion modelling. J Hazard Mater 318:758–771. https://doi.org/10.1016/j.jhazmat.2016.06.015

173. Mouilleau Y, Champassith A (2009) CFD simulations of atmospheric gas dispersion using the fire dynamics simulator (FDS). J Loss Prev Process Ind 22:316–323. https://doi.org/10.1016/j.jlp.2008.11.009

174. Tohidi A, Kaye NB (2017) Stochastic modeling of firebrand shower scenarios. Fire Saf J 91:91–102. https://doi.org/10.1016/j.firesaf.2017.04.039

175. Tohidi A, Kaye NB (2017) Comprehensive wind tunnel experiments of lofting and downwind transport of non-combusting rod-like model firebrands during firebrand shower scenarios. Fire Saf J 90:95–111. https://doi.org/10.1016/j.firesaf.2017.04.032

176. Rios O, Jahn W, Rein G (2014) Forecasting wind-driven wildfires using an inverse modelling approach. Nat Hazards Earth Syst Sci 14:1491–1503. https://doi.org/10.5194/nhess-14-1491-2014

177. Węgrzyński W, Turkowski P (2015) Fire resistance of a roof tensile structure in parametric fire conditions calculated using CFD simulations and simplified calculation methods. In: SFPE Europe conference on fire safety engineering

178. Węgrzyński W, Krajewski G (2015) ITB technical report 2752.3/15/Z00NP